A finite strain rod model that incorporates general cross section deformation and its implementation by the Finite Element Method

Evandro R. Dasambiagio, Paulo M. Pimenta
and Eduardo M. B. Campello

Department of Structural and Geotechnical Engineering, Polytechnic School at the University of São Paulo, São Paulo/SP – Brazil

Abstract

A fully nonlinear geometrically-exact multi-parameter rod model is presented in this work for the analysis of beam structures undergoing arbitrarily large 3-D deformations. Our approach accounts for in-plane distortions of the cross-sections as well as for out-of-plane cross-sectional warping by means of cross-sectional degrees-of-freedom within the rod theory. With such a kinematical description, fully three-dimensional finite-strain constitutive equations are permitted in a totally consistent way. Proper representation of profile (distortional) deformations, which are typical of cold-formed thin-walled beam structures, may be attained and we believe this is a major feature of our formulation. The model is implemented via the finite element method and numerical examples are shown to assess the performance of the scheme.

Keywords: rods, cross-sectional deformations, finite rotations, finite strains, Finite Element Method.

1 Introduction

The main purpose of this work is to (i) present a fully nonlinear geometrically-exact multi-parameter rod model that allows for cross-sectional deformations and (ii) develop its finite element implementation. The formulation can be understood as an extension of our earlier works in [1–4], as presented in [5], in the sense that the restrictions to a rigid cross-section and to a St.-Venant-type elastic warping are now removed from the theory. The ideas for the kinematical description were first set by the authors in [6], however at that time only the general theoretical grounds were discussed and no numerical results were attained. In the present work, we exploit and further develop the concepts presented therein and derive the complete rod theory, together with its numerical implementation via the finite element method and related examples.

We follow a cross-section resultant approach and define the cross-sectional quantities in terms of first Piola-Kichhoff stresses and deformation gradient strains, based on the concept of a cross-section

Mechanics of Solids in Brazil 2009, H.S. da Costa Mattos & Marcílio Alves (Editors)
Brazilian Society of Mechanical Sciences and Engineering, ISBN 978-85-85769-43-7

director. Besides practical importance, the use of cross-sectional resultants simplifies the derivation of equilibrium equations and the enforcement of boundary conditions, in either weak and strong senses. In addition, the corresponding tangent of the weak form is obtained in a more expedient way, rendering always symmetric for hyperelastic materials and conservative loadings even far from equilibrium states.

The definition of a cross-section director plays a central role in our formulation. Accordingly, it allows for the introduction of independent degrees-of-freedom pertaining to the cross-sections to describe both the in-plane cross-sectional distortions and the out-of-plane cross-sectional warping. Fully three-dimensional finite-strain constitutive equations can therefore be adopted with no additional considerations nor condensations. This is a remarkable feature and up to our knowledge makes our model the first rod formulation as to permit general 3-D material laws for arbitrarily large strains. Hyperelasticity and finite elastoplasticity are thus made possible in a consistent way within the context of rods.

The Euler-Rodrigues formula is used to describe finite rotations in a total Lagrangean framework. We assume a straight reference configuration for the rod axis, but initially curved rods can also be considered if regarded as a stress-free deformed state from the straight position (see the ideas of [7, 8]).

Altogether, the present assumptions provide a consistent basis to the computational simulation of profile (distortional) deformations, which are typical of cold-formed thin-walled rod structures. We believe this is one of the major contributions of our work. For a historical background on the subject, we address the interested reader to the papers from [1, 2, 9–18] and references therein.

Throughout the text, italic Latin or Greek lowercase letters $(a, b, \ldots, \alpha, \beta, \ldots)$ denote scalar quantities, bold italic Latin or Greek lowercase letters $(\boldsymbol{a},\ \boldsymbol{b},\ \ldots \boldsymbol{\alpha}, \boldsymbol{\beta}, \ldots)$ denote vectors, bold italic Latin or Greek capital letters $(\boldsymbol{A},\ \boldsymbol{B},\ \ldots)$ denote second-order tensors, bold calligraphic Latin capital letters $(\boldsymbol{\mathcal{A}},\ \boldsymbol{\mathcal{B}},\ \ldots)$ denote third-order tensors and bold blackboard Latin capital letters $(\mathbb{A},\ \mathbb{B},\ \ldots)$ denote fourth-order tensors in a three-dimensional Euclidean space. Vectors and matrices built up of tensor components on orthogonal frames (e.g. for computational purposes) are expressed by boldface upright Latin letters $(\mathbf{A}, \mathbf{B}, \ldots \mathbf{a}, \mathbf{b}, \ldots)$. Summation convention over repeated indices is adopted in the entire text, with Greek indices ranging from 1 to 2 and Latin indices from 1 to 3.

2 The multi-parameter rod theory with general cross-sectional deformations

2.1 Kinematics

It is assumed at the outset that the rod is straight at the initial configuration, which is used as reference. Initially curved rods can be mapped by standard isoparametric means, or can be regarded as a stress-free deformed state from the straight reference position (see [7, 8]).

Let $\{\boldsymbol{e}_1^r, \boldsymbol{e}_2^r, \boldsymbol{e}_3^r\}$ be a local orthonormal system in the reference configuration, with $\boldsymbol{e}_3^r$ placed along the rod axis as depicted in Fig. 1. Cross-sectional planes in this configuration are uniquely defined by the vectors $\boldsymbol{e}_\alpha^r$. The position of the rod material points in the reference configuration can be described by

$$\boldsymbol{\xi} = \boldsymbol{\zeta} + \boldsymbol{a}^r, \tag{1}$$

Mechanics of Solids in Brazil 2009, H.S. da Costa Mattos & Marcílio Alves (Editors)
Brazilian Society of Mechanical Sciences and Engineering, ISBN 978-85-85769-43-7

where

$$\boldsymbol{\zeta} = \zeta \boldsymbol{e}_3^r, \quad \zeta \in \Omega = [0, \ell] \tag{2}$$

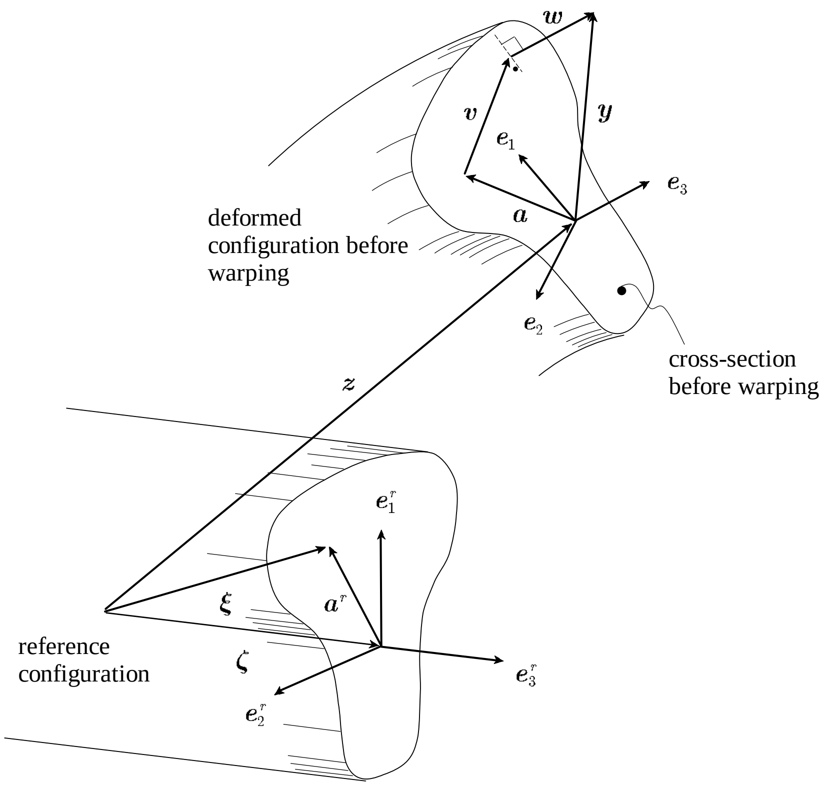

Figure 1: Rod description and basic kinematical quantities.

defines a point on the rod axis and

$$\boldsymbol{a}^r = \xi_\alpha \boldsymbol{e}_\alpha^r \tag{3}$$

is the cross-section director at this point. The axis-coordinate ζ defines the rod length ℓ in the reference configuration. Observe that $\{\xi_1, \xi_2, \zeta\}$ sets a three-dimensional Cartesian frame.

Let now $\{\boldsymbol{e}_1, \boldsymbol{e}_2, \boldsymbol{e}_3\}$ be a local orthonormal system on the current configuration, with $\boldsymbol{e}_\alpha$ attached to the cross-sectional plane before its warping. The rotation of the cross-section in the 3-D space is described by a rotation tensor $\boldsymbol{Q} = \hat{\boldsymbol{Q}}(\zeta)$, such that $\boldsymbol{e}_i = \boldsymbol{Q}\boldsymbol{e}_i^r$. In the current configuration, the position $\boldsymbol{x}$ of the material points (see Fig. 1) is given by the vector field

Mechanics of Solids in Brazil 2009, H.S. da Costa Mattos & Marcílio Alves (Editors)
Brazilian Society of Mechanical Sciences and Engineering, ISBN 978-85-85769-43-7

$$\boldsymbol{x} = \boldsymbol{z} + \boldsymbol{y} \; , \tag{4}$$

where $\boldsymbol{z} = \hat{\boldsymbol{z}}(\zeta)$ represents the current position of a point on the rod axis and $\boldsymbol{y}$ the position of the remaining points on the cross-section relative to the axis. We assume that the cross-sections are first rigidly rotated from the reference configuration, then undergo an in-plane deformation and then are warped in the out-of-plane direction, so that the vector $\boldsymbol{y}$ can be decomposed as follows

$$\boldsymbol{y} = \boldsymbol{a} + \boldsymbol{v} + \boldsymbol{w} \; . \tag{5}$$

Here,

$$\boldsymbol{a} = \boldsymbol{Q}\boldsymbol{a}^r \tag{6}$$

is the current cross-section director, representing the rotational part of the deformation,

$$\boldsymbol{v} = v_\beta \boldsymbol{e}_\beta \tag{7}$$

is the vector of in-plane (or transversal) displacements, describing the in-plane distortions of the cross-section, and

$$\boldsymbol{w} = w\boldsymbol{e}_3 \tag{8}$$

is the vector of out-of-plane displacements, embodying the cross-sectional warping. Notice that first-order shear deformations are accounted for, since $\boldsymbol{e}_3$ is not necessarily coincident with the deformed axis.

Several kinematical assumptions are possible for the vector of transversal displacements $\boldsymbol{v}$. Let $\boldsymbol{r} = \hat{\boldsymbol{r}}(\zeta)$ be a vector that collects the n_v cross-sectional transverse degrees-of-freedom, necessary to describe the cross-sectional in-plane distortions. We assume here that $\boldsymbol{v}$ is a linear function[1] of $\boldsymbol{r}$ such that

$$\boldsymbol{v} = \left(\boldsymbol{e}_\beta \otimes \boldsymbol{\phi}_\beta\right)\boldsymbol{r} \; , \tag{9}$$

where $\boldsymbol{\phi}_\beta = \hat{\boldsymbol{\phi}}_\beta(\xi_\alpha)$ are two vectors of cross-sectional shape functions describing the transversal distribution of the components of $\boldsymbol{v}$ on the cross-section. From (7), these components are given by

$$v_\beta = \boldsymbol{\phi}_\beta \cdot \boldsymbol{r} \; . \tag{10}$$

A number of expressions are possible for $\boldsymbol{\phi}_\beta$, according to the degree of refinement desired for the representation of the cross-sectional distortions. Here we adopt

[1]Nonlinear relations may be necessary for the modeling of local buckling in cold-formed thin-walled metallic profiles. This will be addressed in a forthcoming paper.

$$\boldsymbol{\phi}_1 = \begin{bmatrix} \xi_1 \\ 1/2\xi_1^2 \\ \xi_1\xi_2 \end{bmatrix} , \quad \boldsymbol{\phi}_2 = \begin{bmatrix} \xi_2 \\ \xi_1\xi_2 \\ 1/2\xi_2^2 \end{bmatrix} \quad \text{and} \quad \boldsymbol{r} = \begin{bmatrix} r_1 \\ r_2 \\ r_3 \end{bmatrix} , \tag{11}$$

with quadratic functions on the two local directions $\boldsymbol{e}_\beta$, as this is the simplest kinematical assumption valid for both membrane and bending dominated deformations in isotropic materials. Notice that in this case $n_v = 3$, i.e. three cross-sectional transverse degrees-of-freedom are necessary for the complete description. It is not difficult to realize that r_1 is important for stretching-dominated situations, while r_2 and r_3 are imperative for the bending-dominated ones. Other possibilities for $\boldsymbol{\phi}_\beta$ are discussed in detail in [6].

There is also a number of possible kinematical assumptions for the out-of-plane displacements $\boldsymbol{w}$ due to warping. Analogously to (9), let us write these displacements as

$$\boldsymbol{w} = (\boldsymbol{e}_3 \otimes \boldsymbol{\psi})\, \boldsymbol{p} \,, \tag{12}$$

where $\boldsymbol{p} = \hat{\boldsymbol{p}}(\zeta)$ is a vector that collects the n_w cross-sectional out-of-plane degrees-of-freedom describing the warping of the cross-section, and $\boldsymbol{\psi} = \hat{\boldsymbol{\psi}}(\xi_\alpha)$ is a vector of corresponding warping shape functions ψ_w. According to (12) the component w of (8) on the current local system is given by

$$w = \boldsymbol{\psi} \cdot \boldsymbol{p} \,. \tag{13}$$

Consideration of $\boldsymbol{w}$ is of central importance in torsion- and other shear-dominated deformations. Again, several expressions are possible for $\boldsymbol{\psi}$ and aiming simplicity (but without loss of generality) we assume here that

$$\boldsymbol{\psi} = [\xi_1\xi_2] \quad \text{and} \quad \boldsymbol{p} = [p] \,, \tag{14}$$

i.e. $n_w = 1$ and $p = \hat{p}(\zeta)$ is the only cross-sectional degree-of-freedom describing the warping deformation. It is not difficult to realize that in this case p represents the warping magnitude and $\psi = \xi_1\xi_2$ is the warping shape. Adoption of such a simple shape function for description of the warping may be understood as the simplest choice possible within the theory, and is valid as a first approximation for the warping of any type of cross-section (notice that for rectangular sections the choice in (14) corresponds to the St.-Venant warping function from the Saint-Venant's torsion theory). More elaborated sets for (14) are discussed in [6].

According to Fig. 1, the displacements of the points on the rod axis can be computed by

$$\boldsymbol{u} = \boldsymbol{z} - \boldsymbol{\zeta} \,. \tag{15}$$

The rotation tensor $\boldsymbol{Q}$, describing the rotation of the cross-sections, may be expressed in terms of the Euler rotation vector $\boldsymbol{\theta}$, by means of the well-known Euler-Rodrigues formula

$$\boldsymbol{Q} = \boldsymbol{I} + h_1(\theta)\, \boldsymbol{\Theta} + h_2(\theta)\, \boldsymbol{\Theta}^2 \,. \tag{16}$$

In this case, $\theta = \|\boldsymbol{\theta}\|$ is the true rotation angle and

$$h_1(\theta) = \frac{\sin\theta}{\theta} \quad \text{and} \quad h_2(\theta) = \frac{1}{2}\left(\frac{\sin\theta/2}{\theta/2}\right)^2 \tag{17^2}$$

are two trigonometric functions, with $\boldsymbol{\Theta} = \text{Skew}(\boldsymbol{\theta})$ as the skew-symmetric tensor whose axial vector is $\boldsymbol{\theta}$. Altogether, the components of $\boldsymbol{u}$, $\boldsymbol{\theta}$, $\boldsymbol{r}$ and $\boldsymbol{p}$ on a global Cartesian system constitute the $3+3+n_v+n_w$ parameters (or cross-sectional degrees-of-freedom) of this rod model.

From differentiation of (4) with respect to $\boldsymbol{\xi}$ one can evaluate the deformation gradient $\boldsymbol{F}$. After some algebra one gets

$$\boldsymbol{F} = \boldsymbol{x}_{,\alpha} \otimes \boldsymbol{e}^r_\alpha + \boldsymbol{x}' \otimes \boldsymbol{e}^r_3, \tag{18}$$

where we have used the notation $(\bullet)_{,\alpha} = \partial(\bullet)/\partial\xi_\alpha$ and $(\bullet)' = \partial(\bullet)/\partial\zeta$ for derivatives. With the aid of (4) through (8), the derivatives in (18) are

$$\boldsymbol{x}_{,\alpha} = \boldsymbol{a}_{,\alpha} + \boldsymbol{v}_{,\alpha} + \boldsymbol{w}_{,\alpha} \quad \text{and} \quad \boldsymbol{x}' = \boldsymbol{z}' + \boldsymbol{a}' + \boldsymbol{v}' + \boldsymbol{w}' \ , \tag{19}$$

in which

$$\begin{aligned}
&\boldsymbol{a}_{,\alpha} = \boldsymbol{Q}\boldsymbol{e}^r_\alpha \ , \quad \boldsymbol{v}_{,\alpha} = \left(\boldsymbol{\phi}_{\beta,\alpha} \cdot \boldsymbol{r}\right)\boldsymbol{Q}\boldsymbol{e}^r_\beta \ , \\
&\boldsymbol{w}_{,\alpha} = \left(\boldsymbol{\psi}_{,\alpha} \cdot \boldsymbol{p}\right)\boldsymbol{Q}\boldsymbol{e}^r_3 \ , \quad \boldsymbol{a}' = \boldsymbol{Q}\left(\boldsymbol{\kappa}^r \times \boldsymbol{a}^r\right) \ , \\
&\boldsymbol{v}' = \boldsymbol{Q}\left[\left(\boldsymbol{\phi}_\beta \cdot \boldsymbol{r}'\right)\boldsymbol{e}^r_\beta + \boldsymbol{\kappa}^r \times \boldsymbol{v}^r\right] \quad \text{and} \\
&\boldsymbol{w}' = \boldsymbol{Q}\left[\left(\boldsymbol{\psi} \cdot \boldsymbol{p}'\right)\boldsymbol{e}^r_3 + \boldsymbol{\kappa}^r \times \boldsymbol{w}^r\right] \ ,
\end{aligned} \tag{20}$$

with

$$\boldsymbol{v}^r = v_\beta \boldsymbol{e}^r_\beta = \boldsymbol{Q}^T\boldsymbol{v} \quad \text{and} \quad \boldsymbol{w}^r = w\boldsymbol{e}^r_3 = \boldsymbol{Q}^T\boldsymbol{w} \ . \tag{21}$$

Still in (20), the following vector has been introduced

$$\boldsymbol{\kappa}^r = \boldsymbol{\Gamma}^T\boldsymbol{\theta}' \ , \tag{22}$$

in which

$$\boldsymbol{\Gamma} = \boldsymbol{I} + h_2(\theta)\,\boldsymbol{\Theta} + h_3(\theta)\,\boldsymbol{\Theta}^2 \tag{23}$$

and

$$h_3(\theta) = \frac{1 - h_1(\theta)}{\theta^2} \ . \tag{24}$$

Vector $\boldsymbol{\kappa}^r$ in (22) can be regarded as the back-rotated counterpart of $\boldsymbol{\kappa} = \text{axial}(\boldsymbol{K}) = \boldsymbol{\Gamma}\boldsymbol{\theta}'$, where $\boldsymbol{K} = \boldsymbol{Q}'\boldsymbol{Q}^T$ is a skew-symmetric tensor that shows up in the derivation of expressions (20). One can understand $\boldsymbol{K}$ as the tensor describing the specific rotations of the cross-sections.

[2]Singularities in $h_1(\theta)$ and $h_2(\theta)$ at $\theta = 0$ are straighforwardly removable.

Thus, the deformation gradient may be rewritten as

$$\boldsymbol{F} = \boldsymbol{Q}\left(\boldsymbol{I} + \boldsymbol{\gamma}^r_\alpha \otimes \boldsymbol{e}^r_\alpha + \boldsymbol{\gamma}^r_3 \otimes \boldsymbol{e}^r_3\right) = \boldsymbol{Q}\boldsymbol{F}^r \ , \tag{25}$$

where $\boldsymbol{F}^r = \boldsymbol{I} + \boldsymbol{\gamma}^r_\alpha \otimes \boldsymbol{e}^r_\alpha + \boldsymbol{\gamma}^r_3 \otimes \boldsymbol{e}^r_3$ is called the back-rotated deformation gradient and

$$\begin{aligned} \boldsymbol{\gamma}^r_\alpha &= \left(\boldsymbol{\phi}_{\beta,\alpha} \cdot \boldsymbol{r}\right)\boldsymbol{e}^r_\beta + \left(\boldsymbol{\psi}_{,\alpha} \cdot \boldsymbol{p}\right)\boldsymbol{e}^r_3 \quad \text{and} \\ \boldsymbol{\gamma}^r_3 &= \boldsymbol{\eta}^r + \boldsymbol{\kappa}^r \times \boldsymbol{y}^r + \left(\boldsymbol{\phi}_\beta \cdot \boldsymbol{r}'\right)\boldsymbol{e}^r_\beta + \left(\boldsymbol{\psi} \cdot \boldsymbol{p}'\right)\boldsymbol{e}^r_3 \ . \end{aligned} \tag{26}$$

Here,

$$\boldsymbol{\eta}^r = \boldsymbol{Q}^T\boldsymbol{z}' - \boldsymbol{e}^r_3 \ , \tag{27}$$

and $\boldsymbol{y}^r$ is the back-rotated counterpart of $\boldsymbol{y}$, i.e.

$$\boldsymbol{y}^r = \boldsymbol{a}^r + \boldsymbol{v}^r + \boldsymbol{w}^r = \boldsymbol{Q}^T\boldsymbol{y} \ . \tag{28}$$

It will be clear on next section that vectors $\boldsymbol{\eta}^r$ of (27) and $\boldsymbol{\kappa}^r$ of (22) can be understood as generalized cross-sectional strains.

The material velocity gradient is given by time differentiation of (25) (denoted by a superposed dot) as follows

$$\dot{\boldsymbol{F}} = \boldsymbol{\Omega}\boldsymbol{F} + \boldsymbol{Q}\left(\dot{\boldsymbol{\gamma}}^r_\alpha \otimes \boldsymbol{e}^r_\alpha + \dot{\boldsymbol{\gamma}}^r_3 \otimes \boldsymbol{e}^r_3\right) \ , \tag{29}$$

where $\boldsymbol{\Omega} = \dot{\boldsymbol{Q}}\boldsymbol{Q}^T$ represents the cross-section spin tensor. The spin axial vector $\boldsymbol{\omega}$ is obtained in a similar way as to obtain the axial vector of $\boldsymbol{K}$, i.e. $\boldsymbol{\omega} = \operatorname{axial}(\boldsymbol{\Omega}) = \boldsymbol{\Gamma}\dot{\boldsymbol{\theta}}$. Derivatives $\dot{\boldsymbol{\gamma}}^r_i$ of (29) are computed directly from (26), what yields

$$\begin{aligned} \dot{\boldsymbol{\gamma}}^r_\alpha &= \left(\boldsymbol{e}^r_\beta \otimes \boldsymbol{\phi}_{\beta,\alpha}\right)\dot{\boldsymbol{q}} + \left(\boldsymbol{e}^r_3 \otimes \boldsymbol{\psi}_{,\alpha}\right)\dot{\boldsymbol{p}} \quad \text{and} \\ \dot{\boldsymbol{\gamma}}^r_3 &= \dot{\boldsymbol{\eta}}^r + \dot{\boldsymbol{\kappa}}^r \times \boldsymbol{y}^r + \left[\left(\boldsymbol{\kappa}^r \times \boldsymbol{e}^r_3\right) \otimes \boldsymbol{\psi}\right]\dot{\boldsymbol{p}} + \left(\boldsymbol{e}^r_3 \otimes \boldsymbol{\psi}\right)\dot{\boldsymbol{p}}' + \\ &\quad + \left[\left(\boldsymbol{\kappa}^r \times \boldsymbol{e}^r_\beta\right) \otimes \boldsymbol{\phi}_\beta\right]\dot{\boldsymbol{r}} + \left(\boldsymbol{e}^r_\beta \otimes \boldsymbol{\phi}_\beta\right)\dot{\boldsymbol{r}}' \ . \end{aligned} \tag{30}$$

In order to fully evaluate expressions (30), the time derivatives $\dot{\boldsymbol{\eta}}^r$ and $\dot{\boldsymbol{\kappa}}^r$ are needed. From (27) and (22), after some algebra it is possible to arrive at

$$\dot{\boldsymbol{\eta}}^r = \boldsymbol{Q}^T\left(\dot{\boldsymbol{u}}' + \boldsymbol{Z}'\boldsymbol{\Gamma}\dot{\boldsymbol{\theta}}\right) \quad \text{and} \quad \dot{\boldsymbol{\kappa}}^r = \boldsymbol{Q}^T\left(\boldsymbol{\Gamma}'\dot{\boldsymbol{\theta}} + \boldsymbol{\Gamma}\dot{\boldsymbol{\theta}}'\right) \ , \tag{31}$$

where $\boldsymbol{Z}' = \operatorname{Skew}(\boldsymbol{z}')$ and

$$\begin{aligned} \boldsymbol{\Gamma}' &= h_2(\theta)\,\boldsymbol{\Theta}' + h_3(\theta)\left(\boldsymbol{\Theta}\boldsymbol{\Theta}' + \boldsymbol{\Theta}'\boldsymbol{\Theta}\right) + \\ &\quad + h_4(\theta)\left(\boldsymbol{\theta} \cdot \boldsymbol{\theta}'\right)\boldsymbol{\Theta} + h_5(\theta)\left(\boldsymbol{\theta} \cdot \boldsymbol{\theta}'\right)\boldsymbol{\Theta}^2 \ . \end{aligned} \tag{32}$$

Notice that in (32) $\boldsymbol{\Theta}' = \operatorname{Skew}\left(\boldsymbol{\theta}'\right)$ and

$$h_4(\theta) = \frac{h_1(\theta) - 2h_2(\theta)}{\theta^2} \quad \text{and} \quad h_5(\theta) = \frac{h_2(\theta) - 3h_3(\theta)}{\theta^2} \tag{33[3]}$$

are two additional trigonometric functions.

2.2 Statics

Let the 1st Piola-Kirchhoff stress tensor be written as

$$\boldsymbol{P} = \boldsymbol{Q}\left(\boldsymbol{\tau}_\alpha^r \otimes \boldsymbol{e}_\alpha^r + \boldsymbol{\tau}_3^r \otimes \boldsymbol{e}_3^r\right) \ . \tag{34}$$

The quantities $\boldsymbol{\tau}_i^r$ are back-rotated stress vectors and act on cross-sectional planes whose normals on the reference configuration are $\boldsymbol{e}_i^r$. Expression (34) motivates the definition of a back-rotated 1st Piola-Kirchhoff stress tensor $\boldsymbol{P}^r$, such that

$$\boldsymbol{P}^r = \boldsymbol{Q}^T\boldsymbol{P} = \boldsymbol{\tau}_\alpha^r \otimes \boldsymbol{e}_\alpha^r + \boldsymbol{\tau}_3^r \otimes \boldsymbol{e}_3^r \ . \tag{35}$$

With the expressions for $\boldsymbol{P}$ and $\dot{\boldsymbol{F}}$, it is not difficult to show that the rod internal power per unit reference volume may be written as

$$\boldsymbol{P} : \dot{\boldsymbol{F}} = \boldsymbol{\tau}_\alpha^r \cdot \dot{\boldsymbol{\gamma}}_\alpha^r + \boldsymbol{\tau}_3^r \cdot \dot{\boldsymbol{\gamma}}_3^r \ , \tag{36}$$

where property $\boldsymbol{P}\boldsymbol{F}^T : \boldsymbol{\Omega} = 0$, arising from the local moment balance equation, was utilized. Introducing (30) into (36) and performing some manipulation with the cross products, one gets

$$\begin{aligned} \boldsymbol{P} : \dot{\boldsymbol{F}} = {} & \boldsymbol{\tau}_3^r \cdot \dot{\boldsymbol{\eta}}^r + \left(\boldsymbol{y}^r \times \boldsymbol{\tau}_3^r\right) \cdot \dot{\boldsymbol{\kappa}}^r + \\ & + \left[\left(\boldsymbol{\tau}_\alpha^r \cdot \boldsymbol{e}_3^r\right)\boldsymbol{\psi}_{,\alpha} + \left(\boldsymbol{\tau}_3^r \cdot \boldsymbol{\kappa}^r \times \boldsymbol{e}_3^r\right)\boldsymbol{\psi}\right] \cdot \dot{\boldsymbol{p}} + \left[\left(\boldsymbol{\tau}_3^r \cdot \boldsymbol{e}_3^r\right)\boldsymbol{\psi}\right] \cdot \dot{\boldsymbol{p}}' + \\ & + \left[\left(\boldsymbol{\tau}_\alpha^r \cdot \boldsymbol{e}_\beta^r\right)\boldsymbol{\phi}_{\beta,\alpha} + \left(\boldsymbol{\tau}_3^r \cdot \boldsymbol{\kappa}^r \times \boldsymbol{e}_\beta^r\right)\boldsymbol{\phi}_\beta\right] \cdot \dot{\boldsymbol{r}} + \left[\left(\boldsymbol{\tau}_3^r \cdot \boldsymbol{e}_\beta^r\right)\boldsymbol{\phi}_\beta\right] \cdot \dot{\boldsymbol{r}}' \ . \end{aligned} \tag{37}$$

Integration of (37) over the cross-section provides

$$\int_A \left(\boldsymbol{P} : \dot{\boldsymbol{F}}\right) dA = \boldsymbol{n}^r \cdot \dot{\boldsymbol{\eta}}^r + \boldsymbol{m}^r \cdot \dot{\boldsymbol{\kappa}}^r + \boldsymbol{\pi} \cdot \dot{\boldsymbol{p}} + \boldsymbol{\alpha} \cdot \dot{\boldsymbol{p}}' + \boldsymbol{\rho} \cdot \dot{\boldsymbol{r}} + \boldsymbol{\beta} \cdot \dot{\boldsymbol{r}}' \ , \tag{38}$$

in which

$$\begin{aligned} & \boldsymbol{n}^r = \textstyle\int_A \boldsymbol{\tau}_3^r dA \ , \quad \boldsymbol{m}^r = \int_A \left(\boldsymbol{y}^r \times \boldsymbol{\tau}_3^r\right) dA \ , \\ & \boldsymbol{\pi} = \textstyle\int_A \left[\left(\boldsymbol{\tau}_\alpha^r \cdot \boldsymbol{e}_3^r\right)\boldsymbol{\psi}_{,\alpha} + \left(\boldsymbol{\tau}_3^r \cdot \boldsymbol{\kappa}^r \times \boldsymbol{e}_3^r\right)\boldsymbol{\psi}\right] dA \ , \quad \boldsymbol{\alpha} = \int_A \left[\left(\boldsymbol{\tau}_3^r \cdot \boldsymbol{e}_3^r\right)\boldsymbol{\psi}\right] dA \ , \\ & \boldsymbol{\rho} = \textstyle\int_A \left[\left(\boldsymbol{\tau}_\alpha^r \cdot \boldsymbol{e}_\beta^r\right)\boldsymbol{\phi}_{\beta,\alpha} + \left(\boldsymbol{\tau}_3^r \cdot \boldsymbol{\kappa}^r \times \boldsymbol{e}_\beta^r\right)\boldsymbol{\phi}_\beta\right] dA \quad \text{and} \\ & \boldsymbol{\beta} = \textstyle\int_A \left[\left(\boldsymbol{\tau}_3^r \cdot \boldsymbol{e}_\beta^r\right)\boldsymbol{\phi}_\beta\right] dA \end{aligned} \tag{39}$$

are the generalized cross-sectional stresses energetically conjugated to the cross-sectional strains $\boldsymbol{\eta}^r$, $\boldsymbol{\kappa}^r$, $\boldsymbol{p}$, $\boldsymbol{p}'$, $\boldsymbol{r}$ and $\boldsymbol{r}'$. In this case, $\boldsymbol{n}^r$ is said to be the back-rotated cross-sectional forces and $\boldsymbol{m}^r$ the back-rotated cross-sectional moments (notice the effect of the in-plane-distortions and of the out-of-plane

[3]The singularities in $h_4(\theta)$ and $h_5(\theta)$ are also removable.

warping on the definition of $\boldsymbol{m}^r$). Vector $\boldsymbol{\pi}$ represents the axial bi-shears, $\boldsymbol{\alpha}$ the axial bi-moments, $\boldsymbol{\rho}$ the transversal bi-shears and $\boldsymbol{\beta}$ the transversal bi-moments.

It is important to remark that $\boldsymbol{\tau}_i^r$, γ_i^r, $\boldsymbol{n}^r$, $\boldsymbol{m}^r$, $\boldsymbol{\eta}^r$, $\boldsymbol{\kappa}^r$, $\boldsymbol{p}$, $\boldsymbol{r}$, $\boldsymbol{\pi}$, $\boldsymbol{\alpha}$, $\boldsymbol{\rho}$ and $\boldsymbol{\beta}$ are not affected by superimposed rigid body motions and in this sense entirely fulfill objectivity requirements. We now collect these cross-sectional quantities into three vectors, as displayed below

$$\boldsymbol{\sigma} = \begin{bmatrix} \boldsymbol{n}^r \\ \boldsymbol{m}^r \\ \boldsymbol{\pi} \\ \boldsymbol{\alpha} \\ \boldsymbol{\rho} \\ \boldsymbol{\beta} \end{bmatrix}, \quad \boldsymbol{\varepsilon} = \begin{bmatrix} \boldsymbol{\eta}^r \\ \boldsymbol{\kappa}^r \\ \boldsymbol{p} \\ \boldsymbol{p}' \\ \boldsymbol{r} \\ \boldsymbol{r}' \end{bmatrix} \quad \text{and} \quad \boldsymbol{d} = \begin{bmatrix} \boldsymbol{u} \\ \boldsymbol{\theta} \\ \boldsymbol{p} \\ \boldsymbol{r} \end{bmatrix}. \tag{40}$$

Note that both $\boldsymbol{\sigma}$ and $\boldsymbol{\varepsilon}$ have $6 + 2(n_v + n_w)$ elements, whilst $\boldsymbol{d}$ encompasses the $6 + n_v + n_w$ cross-sectional degrees-of-freedom. Definitions in (40) allow us to write (38) as follows

$$\int_A \left(\boldsymbol{P} : \dot{\boldsymbol{F}}\right) dA = \boldsymbol{\sigma} \cdot \dot{\boldsymbol{\varepsilon}}\,. \tag{41}$$

Here, the time derivative $\dot{\boldsymbol{\varepsilon}}$ may be written in a very compact manner as

$$\dot{\boldsymbol{\varepsilon}} = \boldsymbol{\Psi}\boldsymbol{\Delta}\dot{\boldsymbol{d}}\,, \tag{42}$$

where

$$\boldsymbol{\Psi} = \begin{bmatrix} \bar{\boldsymbol{\Psi}} & \boldsymbol{O}_{6\times 2(n_v+n_w)} \\ \boldsymbol{O}_{2(n_v+n_w)\times 9} & \boldsymbol{I}_{2(n_v+n_w)} \end{bmatrix} \quad \text{and} \quad \boldsymbol{\Delta} = \begin{bmatrix} \bar{\boldsymbol{\Delta}} & \boldsymbol{O}_{9\times n_w} & \boldsymbol{O}_{9\times n_v} \\ \boldsymbol{O}_{n_w\times 9} & \boldsymbol{I}_{n_w} & \boldsymbol{O}_{n_w\times n_v} \\ \boldsymbol{O}_{n_w\times 9} & \boldsymbol{I}_{n_w}\frac{\partial}{\partial\zeta} & \boldsymbol{O}_{n_w\times n_v} \\ \boldsymbol{O}_{n_v\times 9} & \boldsymbol{O}_{n_v\times n_w} & \boldsymbol{I}_{n_v} \\ \boldsymbol{O}_{n_v\times 9} & \boldsymbol{O}_{n_v\times n_w} & \boldsymbol{I}_{n_v}\frac{\partial}{\partial\zeta} \end{bmatrix} \tag{43}$$

are respectively a $[6 + 2(n_v + n_w)] \times [9 + 2(n_v + n_w)]$ linear operator and a $[9 + 2(n_v + n_w)] \times (6 + n_v + n_w)$ differential operator. In (43) one has

$$\bar{\boldsymbol{\Psi}} = \begin{bmatrix} \boldsymbol{Q}^T & \boldsymbol{O} & \boldsymbol{Q}^T\boldsymbol{Z}'\boldsymbol{\Gamma} \\ \boldsymbol{O} & \boldsymbol{Q}^T\boldsymbol{\Gamma} & \boldsymbol{Q}^T\boldsymbol{\Gamma}' \end{bmatrix}_{6\times 9} \quad \text{and} \quad \bar{\boldsymbol{\Delta}} = \begin{bmatrix} \boldsymbol{I}\frac{\partial}{\partial\zeta} & \boldsymbol{O} \\ \boldsymbol{O} & \boldsymbol{I}\frac{\partial}{\partial\zeta} \\ \boldsymbol{O} & \boldsymbol{I} \end{bmatrix}_{9\times 6}, \tag{44}$$

which correspond exactly to $\boldsymbol{\Psi}$ and $\boldsymbol{\Delta}$ of [1–4].

With (41) at hand, the rod internal power on a domain $\Omega = [0, \ell]$ is then given by

$$P_{int} = \int_{\Omega} (\boldsymbol{\sigma} \cdot \dot{\boldsymbol{\varepsilon}})\, d\zeta \; . \tag{45}$$

The external power on the same domain $\Omega = [0, \ell]$ can be expressed by

$$P_{\text{ext}} = \int_{\Omega} \left(\int_{\Gamma} \boldsymbol{t} \cdot \dot{\boldsymbol{x}} d\Gamma + \int_{A} \boldsymbol{b} \cdot \dot{\boldsymbol{x}} dA \right) d\zeta \; , \tag{46}$$

where Γ is the contour of a cross-section, $\boldsymbol{t}$ is the external surface traction per unit reference area and $\boldsymbol{b}$ is the vector of body forces per unit reference volume. By time differentiation of (4), one has

$$\dot{\boldsymbol{x}} = \dot{\boldsymbol{u}} + \boldsymbol{\omega} \times \boldsymbol{y} + \left(\boldsymbol{e}_{\beta} \otimes \boldsymbol{\varphi}_{\beta} \right) \dot{\boldsymbol{r}} \; + (\boldsymbol{e}_3 \otimes \boldsymbol{\psi})\, \dot{\boldsymbol{p}} \; , \tag{47}$$

which can be introduced into (46) so that

$$P_{\text{ext}} = \int_{\Omega} \left(\bar{\boldsymbol{q}} \cdot \dot{\boldsymbol{d}} \right) d\zeta \; , \tag{48}$$

where

$$\bar{\boldsymbol{q}} = \begin{bmatrix} \bar{\boldsymbol{n}} \\ \bar{\boldsymbol{\mu}} \\ \bar{\boldsymbol{\alpha}} \\ \bar{\boldsymbol{\beta}} \end{bmatrix} . \tag{49}$$

In this expression the following generalized external forces have been introduced

$$\begin{aligned} &\bar{\boldsymbol{n}} = \textstyle\int_{\Gamma} \boldsymbol{t} d\Gamma + \int_{A} \boldsymbol{b} dA \; , \\ &\bar{\boldsymbol{\mu}} = \boldsymbol{\Gamma}^T \bar{\boldsymbol{m}} \; , \quad \text{with} \quad \bar{\boldsymbol{m}} = \textstyle\int_{\Gamma} \boldsymbol{y} \times \boldsymbol{t} d\Gamma + \int_{A} \boldsymbol{y} \times \boldsymbol{b} dA \; , \\ &\bar{\boldsymbol{\alpha}} = \textstyle\int_{\Gamma} (\boldsymbol{e}_3 \cdot \boldsymbol{t})\, \boldsymbol{\psi} d\Gamma + \int_{A} (\boldsymbol{e}_3 \cdot \boldsymbol{b})\, \boldsymbol{\psi} dA \quad \text{and} \\ &\bar{\boldsymbol{\beta}} = \textstyle\int_{\Gamma} (\boldsymbol{e}_{\beta} \cdot \boldsymbol{t})\, \boldsymbol{\phi}_{\beta} d\Gamma + \int_{A} (\boldsymbol{e}_{\beta} \cdot \boldsymbol{b})\, \boldsymbol{\phi}_{\beta} dA \; , \end{aligned} \tag{50}$$

where $\bar{\boldsymbol{n}}$ is the applied external force, $\bar{\boldsymbol{m}}$ the applied external moment, $\bar{\boldsymbol{\alpha}}$ the applied external axial bi-moments and $\bar{\boldsymbol{\beta}}$ the applied external transversal bi-moments, all per unit length of the rod axis in the reference configuration.

2.3 Equilibrium

In the same way as to obtain (45), one can have the expression for the rod internal virtual work on a domain $\Omega = [0, \ell]$ as follows

$$\delta W_{int} = \int_{\Omega} (\boldsymbol{\sigma} \cdot \delta\boldsymbol{\varepsilon})\, d\zeta \; , \quad \text{with} \quad \delta\boldsymbol{\varepsilon} = \boldsymbol{\Psi}\boldsymbol{\Delta}\delta\boldsymbol{d} \; . \tag{51}$$

The external virtual work on the same domain $\Omega = [0, \ell]$ may be evaluated similarly to (48), i.e.

$$\delta W_{\text{ext}} = \int_{\Omega} (\bar{\boldsymbol{q}} \cdot \delta \boldsymbol{d}) \, d\zeta \ , \tag{52}$$

so that the rod local equilibrium can be stated by means of the virtual work theorem in a standard way:

$$\delta W = \delta W_{\text{int}} - \delta W_{\text{ext}} = 0 \quad \text{in } \Omega, \quad \forall \delta \boldsymbol{d} \ . \tag{53}$$

Introducing (51) and (52) into this expression, and performing partial integration on the terms with $\delta \boldsymbol{u}'$, $(\boldsymbol{\Gamma} \delta \boldsymbol{\theta})'$, $\delta \boldsymbol{p}'$ and $\delta \boldsymbol{r}'$, the following local equilibrium equations in Ω are obtained by standard arguments of variational calculus

$$\boldsymbol{n}' + \bar{\boldsymbol{n}} = \boldsymbol{o} \ , \tag{54a}$$

$$\boldsymbol{m}' + \boldsymbol{z}' \times \boldsymbol{n} + \bar{\boldsymbol{m}} = \boldsymbol{o} \ , \tag{54b}$$

$$\boldsymbol{\alpha}' - \boldsymbol{\pi} + \bar{\boldsymbol{\alpha}} = \boldsymbol{o} \quad \text{and} \tag{54c}$$

$$\boldsymbol{\beta}' - \boldsymbol{\rho} + \bar{\boldsymbol{\beta}} = \boldsymbol{o} \ . \tag{54d}$$

Here,

$$\boldsymbol{n} = \boldsymbol{Q}\boldsymbol{n}^r \quad \text{and} \quad \boldsymbol{m} = \boldsymbol{Q}\boldsymbol{m}^r \tag{55}$$

are the true cross-sectional force and couple resultants with respect to the current configuration. Equations (54a) and (54b) could be obtained by Statics as well.

The essential boundary conditions emanating from (53) are prescribed in terms of $\boldsymbol{d}$, i.e. $\boldsymbol{u}$, $\boldsymbol{\theta}$, $\boldsymbol{p}$ and $\boldsymbol{r}$. On the other hand, the natural boundary conditions are prescribed in terms of the static quantities $\boldsymbol{n}$, $\boldsymbol{\mu} = \boldsymbol{\Gamma}^T \boldsymbol{m}$, $\boldsymbol{\alpha}$ and $\boldsymbol{\beta}$. We draw the attention of the reader to fact that the pseudo-moment $\boldsymbol{\mu} = \boldsymbol{\Gamma}^T \boldsymbol{m}$ must be prescribed, and not purely $\boldsymbol{m}$ as one would expect.

2.4 Tangent of the weak form

The Gateaux derivative of δW in (53) with respect to $\boldsymbol{d}$, after some laborious manipulation, leads to the tangent bilinear form

$$\delta\,(\delta W) = \int_{\Omega} \left[(\boldsymbol{\Psi} \boldsymbol{\Delta} \delta \boldsymbol{d}) \cdot (\boldsymbol{D} \boldsymbol{\Psi} \boldsymbol{\Delta} \delta \boldsymbol{d}) + (\boldsymbol{\Delta} \delta \boldsymbol{d}) \cdot (\boldsymbol{G} \boldsymbol{\Delta} \delta \boldsymbol{d}) - \delta \boldsymbol{d} \cdot (\boldsymbol{L} \delta \boldsymbol{d}) \right] d\Omega \ , \tag{56}$$

in which

$$\boldsymbol{D} = \frac{\partial \boldsymbol{\sigma}}{\partial \boldsymbol{\varepsilon}} \ , \quad \boldsymbol{G} = \begin{bmatrix} \bar{\boldsymbol{G}} & \boldsymbol{O}_{9 \times 2(n_v + n_w)} \\ \boldsymbol{O}_{2(n_v + n_w) \times 9} & \boldsymbol{O}_{2(n_v + n_w) \times 2(n_v + n_w)} \end{bmatrix} \quad \text{and} \quad \boldsymbol{L} = \frac{\partial \bar{\boldsymbol{q}}}{\partial \boldsymbol{d}} \ . \tag{57}$$

Operators $\boldsymbol{D}$ and $\boldsymbol{G}$ represent the constitutive contribution and the geometrical effects of the internal forces on the tangent operator, respectively. It is worth mentioning that operator $\bar{\boldsymbol{G}}$ in (57) is identical to $\boldsymbol{G}$ of [1, 2] (where it was first derived, see appendix A for more details), what remarkably means that the consideration of cross-sectional in-plane distortions and out-of-plane warping does not introduce any additional geometric terms into (56). Consequently, $\boldsymbol{G}$ is a function of $\boldsymbol{n}^r$, $\boldsymbol{m}^r$, $\boldsymbol{u}$ and $\boldsymbol{\theta}$ only, remaining always symmetric even far from equilibrium states. Operator $\boldsymbol{L}$, however, stands for the geometrical effects of the external forces and depends directly on the character of the external loading, as one can see in (57)[4]. The bilinear form (56) is therefore symmetric whenever $\boldsymbol{D} = \boldsymbol{D}^T$ and $\boldsymbol{L} = \boldsymbol{L}^T$, i.e. whenever the material is hyperelastic (or whenever the stress integration algorithm for inelastic materials possesses a potential) and the external loading is locally conservative.

We introduce now the following tensors of elastic (or algorithmic) tangent moduli

$$\frac{\partial \boldsymbol{\tau}_i^r}{\partial \boldsymbol{\gamma}_j^r} = \boldsymbol{C}_{ij} \ . \tag{58}$$

With the aid of (58), together with the derivatives

$$\begin{aligned}
&\frac{\partial \boldsymbol{\gamma}_\alpha^r}{\partial \boldsymbol{\eta}^r} = \boldsymbol{O} \ , && \frac{\partial \boldsymbol{\gamma}_3^r}{\partial \boldsymbol{\eta}^r} = \boldsymbol{I} \ , \\
&\frac{\partial \boldsymbol{\gamma}_\alpha^r}{\partial \boldsymbol{\kappa}^r} = \boldsymbol{O} \ , && \frac{\partial \boldsymbol{\gamma}_3^r}{\partial \boldsymbol{\kappa}^r} = -\boldsymbol{Y}^r , \\
&\frac{\partial \boldsymbol{\gamma}_\alpha^r}{\partial \boldsymbol{p}} = \boldsymbol{e}_3^r \otimes \boldsymbol{\psi}_{,\alpha} \ , && \frac{\partial \boldsymbol{\gamma}_3^r}{\partial \boldsymbol{p}} = (\boldsymbol{\kappa}^r \times \boldsymbol{e}_3^r) \otimes \boldsymbol{\psi} \ , \\
&\frac{\partial \boldsymbol{\gamma}_\alpha^r}{\partial \boldsymbol{p}'} = \boldsymbol{O} \ , && \frac{\partial \boldsymbol{\gamma}_3^r}{\partial \boldsymbol{p}'} = \boldsymbol{e}_3^r \otimes \boldsymbol{\psi} \ , \\
&\frac{\partial \boldsymbol{\gamma}_\alpha^r}{\partial \boldsymbol{r}} = \boldsymbol{e}_\beta^r \otimes \boldsymbol{\phi}_{\beta,\alpha} \ , && \frac{\partial \boldsymbol{\gamma}_3^r}{\partial \boldsymbol{r}} = \left(\boldsymbol{\kappa}^r \times \boldsymbol{e}_\beta^r\right) \otimes \boldsymbol{\phi}_\beta \quad \text{and} \\
&\frac{\partial \boldsymbol{\gamma}_\alpha^r}{\partial \boldsymbol{r}'} = \boldsymbol{O} \ , && \frac{\partial \boldsymbol{\gamma}_3^r}{\partial \boldsymbol{r}'} = \boldsymbol{e}_\beta^r \otimes \boldsymbol{\phi}_\beta \ ,
\end{aligned} \tag{59}$$

where $\boldsymbol{Y}^r = \text{Skew}(\boldsymbol{y}^r)$, one can obtain the elements of $\boldsymbol{D}$ (see appendix B) by the chain rule. We remark that $\boldsymbol{D}$ is symmetric as long as

$$\boldsymbol{C}_{ij} = \boldsymbol{C}_{ji}^T \ . \tag{60}$$

3 Elastic constitutive equations

We assume the rod is made of a hyperelastic material that may undergo arbitrarily large strains. With this assumption, the developments presented in this section are general in the sense that they are derived for fully three-dimensional finite strain constitutive models. These achievements are only possible due to the three-dimensional character of our rod theory, which allows for a complete three-dimensional state of deformation for a point within the rod body. Objectivity requirements (in the

[4] More details on the operator $\boldsymbol{L}$ can be found in appendix C.

sense of [19, 20]) are automatically fulfilled by the use of objective strain measures. Extension to finite elastoplasticity is straightforward once a stress integration scheme within a time step is at hand.

3.1 General hyperelastic materials

We write the symmetric Green-Lagrange strain tensor as

$$\boldsymbol{E} = \frac{1}{2}\left(\boldsymbol{C} - \boldsymbol{I}\right) \ , \tag{61}$$

where

$$\boldsymbol{C} = \boldsymbol{F}^T\boldsymbol{F} = \left(\boldsymbol{F}^r\right)^T \boldsymbol{F}^r \tag{62}$$

is the right Cauchy-Green strain tensor. The second Piola-Kirchhoff stress tensor $\boldsymbol{S}$ is energetically conjugated to $\boldsymbol{E}$ and is such that $\boldsymbol{P} = \boldsymbol{F}\boldsymbol{S}$, or equivalently

$$\boldsymbol{P}^r = \boldsymbol{F}^r\boldsymbol{S}. \tag{63}$$

A general hyperelastic material can be fully described by a specific strain energy function $\psi = \hat{\psi}\left(\boldsymbol{E}\right)$, such that $\boldsymbol{S}$ is given by

$$\boldsymbol{S} = \frac{\partial \psi}{\partial \boldsymbol{E}} \ . \tag{64}$$

As a consequence, a fourth-order tensor of elastic tangent moduli for the pair $\{\boldsymbol{S}, \boldsymbol{E}\}$ can be defined as

$$\mathbb{D} = \frac{\partial \boldsymbol{S}}{\partial \boldsymbol{E}} = \frac{\partial^2 \psi}{\partial \boldsymbol{E}^2} \ . \tag{65}$$

With the aid of the following third-order tensors

$$\boldsymbol{\mathcal{B}}_i = \frac{\partial \boldsymbol{E}}{\partial \gamma_i^r} \ , \tag{66}$$

the relations

$$\boldsymbol{\tau}_i^r = \boldsymbol{\mathcal{B}}_i^T\boldsymbol{S} \tag{67}$$

can be readily derived from (63). From these last three expressions, and from (58), we arrive at

$$\boldsymbol{C}_{ij} = \boldsymbol{\mathcal{B}}_i^T\mathbb{D}\boldsymbol{\mathcal{B}}_j + \left(\boldsymbol{e}_i^r \cdot \boldsymbol{S}\boldsymbol{e}_j^r\right)\boldsymbol{I} \ , \tag{68}$$

with which $\boldsymbol{D}$ can be computed.

3.2 Isotropic hyperelastic materials

For isotropic hyperelasticity, the strain energy function ψ can be written in terms of the invariants of the right Cauchy-Green strain tensor $\boldsymbol{C}$. We adopt here the following set of invariants

$$I_1 = \boldsymbol{I} : \boldsymbol{C} \ , \quad I_2 = \frac{1}{2}\boldsymbol{I} : \boldsymbol{C}^2 \quad \text{and} \quad J = \det \boldsymbol{F} \ , \tag{69}$$

with which we write $\psi = \hat{\psi}\,(I_1, I_2, J)$. Using (63) and (64), the back-rotated first Piola-Kirchhoff stress tensor is then obtained via

$$\boldsymbol{P}^r = 2\boldsymbol{F}^r \left(\frac{\partial \psi}{\partial \boldsymbol{C}}\right) \ , \tag{70}$$

what yields

$$\boldsymbol{P}^r = \frac{\partial \psi}{\partial J} J(\boldsymbol{F}^r)^{-T} + 2\boldsymbol{F}^r \left(\frac{\partial \psi}{\partial I_1}\boldsymbol{I} + \frac{\partial \psi}{\partial I_2}\boldsymbol{C}\right) \tag{71}$$

if the chain rule is applied with the derivatives

$$\frac{\partial J}{\partial \boldsymbol{C}} = \frac{1}{2} J \boldsymbol{C}^{-1} \ , \quad \frac{\partial I_1}{\partial \boldsymbol{C}} = \boldsymbol{I} \quad \text{and} \quad \frac{\partial I_2}{\partial \boldsymbol{C}} = \boldsymbol{C} \ . \tag{72}$$

Conversely, as one can readily verify, if we write the back-rotated deformation gradient as

$$\boldsymbol{F}^r = \boldsymbol{f}_i^r \otimes \boldsymbol{e}_i^r \ , \tag{73}$$

where $\boldsymbol{f}_i^r = \boldsymbol{e}_i^r + \boldsymbol{\gamma}_i^r$ (see expression (25)), then

$$\begin{aligned} &J = (\boldsymbol{f}_1^r \times \boldsymbol{f}_2^r) \cdot \boldsymbol{f}_3^r \ , \\ &J(\boldsymbol{F}^r)^{-T} = \boldsymbol{g}_i^r \otimes \boldsymbol{e}_i^r \quad \text{and} \\ &\boldsymbol{F}^r\boldsymbol{C} = \left(\boldsymbol{f}_i^r \cdot \boldsymbol{f}_j^r\right) \boldsymbol{f}_i^r \otimes \boldsymbol{e}_j^r \ , \end{aligned} \tag{74}$$

in which

$$\boldsymbol{g}_1^r = \boldsymbol{f}_2^r \times \boldsymbol{f}_3^r \ , \quad \boldsymbol{g}_2^r = \boldsymbol{f}_3^r \times \boldsymbol{f}_1^r \quad \text{and} \quad \boldsymbol{g}_3^r = \boldsymbol{f}_1^r \times \boldsymbol{f}_2^r \ . \tag{75}$$

Introducing (74) into (71), one arrives at the following expression for the vector-columns of $\boldsymbol{P}^r$:

$$\boldsymbol{\tau}_i^r = \frac{\partial \psi}{\partial J}\boldsymbol{g}_i^r + 2\frac{\partial \psi}{\partial I_1}\boldsymbol{f}_i^r + 2\frac{\partial \psi}{\partial I_2}\left(\boldsymbol{f}_j^r \otimes \boldsymbol{f}_j^r\right)\boldsymbol{f}_i^r \ . \tag{76}$$

3.3 A neo-Hookean isotropic hyperelastic material

A simple poly-convex neo-Hookean material as proposed in [20, 21] is represented by the specific strain energy function

$$\psi\left(J, I_1\right)=\frac{1}{2}\lambda\left[\frac{1}{2}\left(J^2-1\right)-\ln J\right]+\frac{1}{2}\mu\left(I_1-3-2\ln J\right) \ , \tag{77}$$

in which λ and μ are material parameters (or Lamé coefficients). With this expression at hand, from (76) we get

$$\tau_i^r=\frac{1}{J}\left[\lambda\frac{1}{2}\left(J^2-1\right)-\mu\right]\boldsymbol{g}_i^r+\mu\boldsymbol{f}_i^r \ , \tag{78}$$

and then the tangent tensors of (58) are given by

$$\begin{aligned}\boldsymbol{C}_{ij}=&\left[\tfrac{1}{2}\lambda\left(1+\tfrac{1}{J^2}\right)+\tfrac{1}{J^2}\mu\right]\boldsymbol{g}_i^r\otimes\boldsymbol{g}_j^r+\mu\,\delta_{ij}\boldsymbol{I}+\\ &-\tfrac{1}{J}\left[\lambda\tfrac{1}{2}\left(J^2-1\right)-\mu\right]\varepsilon_{ijk}\,\mathrm{Skew}\left(\boldsymbol{f}_k^r\right) \ .\end{aligned} \tag{79}$$

Here, $\delta_{ij}=\boldsymbol{e}_i^r\cdot\boldsymbol{e}_j^r$ and $\varepsilon_{ijk}=\boldsymbol{e}_i^r\cdot\boldsymbol{e}_j^r\times\boldsymbol{e}_k^r$ are the usual Kronecker and permutation symbols, respectively. From (79), the constitutive matrix $\boldsymbol{D}$ can be computed.

4 Finite Element implementation

The description of the rod deformation generates a boundary value problem whose weak form (53) can be solved by several approximation techniques. We adopt here a Galerkin type of approximation, the trial functions of which are to be supplied by the finite element method. We write the finite element interpolation in a particular element e, $e=1,\ldots N_e$, as follows

$$\boldsymbol{d}=\mathbf{N}\mathbf{p}_e \ , \tag{80}$$

where $\mathbf{N}$ is the matrix of element shape functions and $\mathbf{p}_e$ the vector of element nodal degrees-of-freedom. The vector of the residual nodal forces for a particular element is then obtained from (80) into (53), and after some algebra one gets

$$\mathbf{P}_e=\int_{\Omega_e}\left[\mathbf{N}^T\bar{\boldsymbol{q}}-\left(\boldsymbol{\Psi}\boldsymbol{\Delta}\mathbf{N}\right)^T\boldsymbol{\sigma}\right]d\zeta \ , \tag{81}$$

in which Ω_e is the element domain. The element tangent stiffness matrix is obtained by inserting (80) into (56), leading to

$$\mathbf{k}_e=\int_{\Omega_e}\left[\left(\boldsymbol{\Psi}\boldsymbol{\Delta}\mathbf{N}\right)^T\boldsymbol{D}\left(\boldsymbol{\Psi}\boldsymbol{\Delta}\mathbf{N}\right)+\left(\boldsymbol{\Delta}\mathbf{N}\right)^T\boldsymbol{G}\left(\boldsymbol{\Delta}\mathbf{N}\right)-\mathbf{N}^T\boldsymbol{L}\mathbf{N}\right]d\zeta \ . \tag{82}$$

Here it is important to remark that the linearization stated in (82) can be performed either before or after discretization. Assemblage of the global residual forces and of the global tangent stiffness may be done as usual by means of

$$\mathbf{R} = \sum_{e=1}^{N_e} \mathbf{A}_e^T \mathbf{P}_e \quad \text{and} \quad \mathbf{K} = \sum_{e=1}^{N_e} \mathbf{A}_e^T \mathbf{k}_e \mathbf{A}_e \ , \tag{83}$$

respectively, where $\mathbf{A}_e$ is the connectivity matrix relating the element nodal degrees-of-freedom $\mathbf{p}_e$ with the whole domain nodal degrees-of-freedom $\mathbf{r}$, i.e.

$$\mathbf{p}_e = \mathbf{A}_e \mathbf{r} \ . \tag{84}$$

Equilibrium is then stated by vanishing the global residual forces,

$$\mathbf{R}(\mathbf{r}) = \boldsymbol{o} \ , \tag{85}$$

what can be iteratively solved by the Newton method for the free degrees-of-freedom.

5 Numerical examples

The finite element expressions derived on the previous section were implemented into a finite element code and in the present section we assess the performance of our formulation by means of two numerical examples. Standard quadratic shape functions of Lagrangian type are adopted to construct $\mathbf{N}$. Reduced gaussian quadrature for computation of (81) and (82) is utilized, whereas integration of the constitutive equation over the cross-sections (i.e. integration of the expressions in appendix B) is performed using a 2×2 gaussian scheme. We remark that several other examples can be found in [5].

5.1 Example 1: pure stretching of a bar

A straight rod with free ends and rectangular cross-section $b \times h$ is subjected to a large tensile normal force $P = 3.75 \times 10^6$ as depicted in Fig. 2. With this example we want to show the ability of the formulation in capturing Poisson's effect when finite stretching occurs. The rod is discretized using four 3-noded elements along with symmetry conditions. We adopt $\nu = 0.499999$ in order to simulate incompressibility. In Fig. 2 one can see the deformed configuration obtained in true scale, and the final dimensions of the cross-sections are also shown (no in-plane distortion is observed as only homothetic deformation occurs). We remark that the rod volume is perfectly preserved, with $J = \det \boldsymbol{F} = 1.0$ being exactly attained in all elements at every converged configuration of the Newton iterations.

5.2 Example 2: pure bending of a bar

The simply supported rod with geometric and material properties shown in Fig. 3 is subjected to a pair of external bending moments M at both ends. The right end support is free to move in the horizontal direction and we apply M such that the rod undergoes a complete round-turn. Discretization is performed using four 3-noded elements, the same as in the previous example. In Fig. 4 one can see a graph of the end moments M against (i) the rotations θ in radians of the right-end section, (ii) the horizontal displacements u of the right-end and (iii) the mid-span vertical displacements v. A plot of

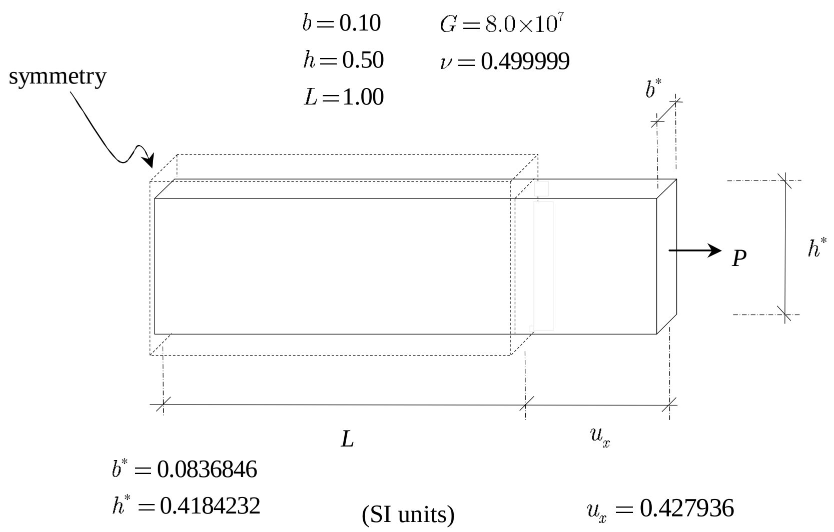

Figure 2: Pure stretching of a bar.

the deformed cross-sections is shown in Fig. 5 for $M = 1.4875 \times 10^6$, where a slight amplification factor is adopted to make the in-plane deformations visible. Notice that the deformation of the cross-sections is nearly the same along the rod's length. Notice, also, that the upper portion of the sections remains distented whereas the bottom part is shortened, as expected. Excellent convergence is found within the Newton solution procedure.

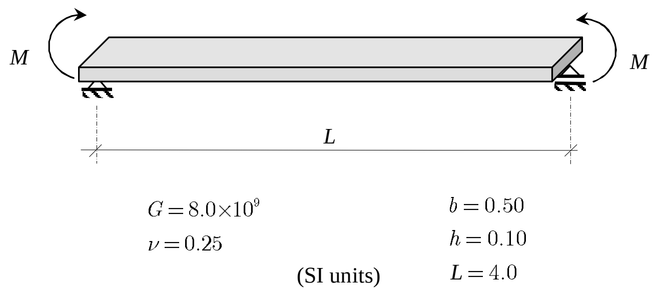

Figure 3: Pure bending of a bar.

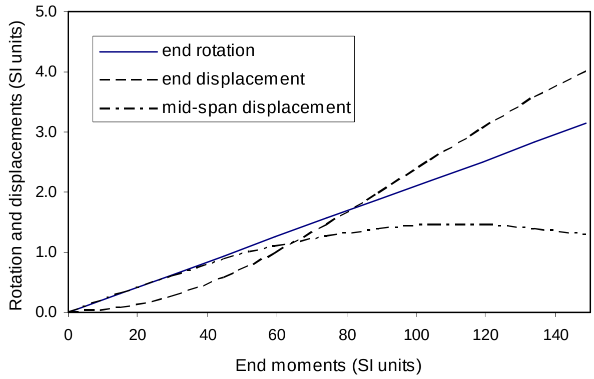

Figure 4: Displacements and rotation at pure bending of a bar.

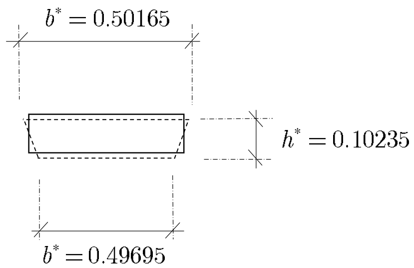

Figure 5: Cross section in-plane deformation at final moment for the pure bending of a bar.

6 Conclusions

In this work we revisit the geometrically-exact six-parameter rod model presented in [1–4] and extend it to a multi-parameter formulation that allows for general cross-sectional in-plane distortions and general out-of-plane warping. We start from the ideas set by the authors in [6], and derive the complete rod theory together with its numerical implementation via the finite element method. The key aspects are the definition of additional degrees of freedom pertaining to the cross-sections and the concept of a cross-section director. We follow a stress-resultant approach, with the cross-sectional resultants being defined based on first Piola-Kirchhoff stresses and deformation gradient strains. Finite rotations are described in a total Lagrangian way. The theory allows for a complete three-dimensional state of deformation for a point within the rod body and for this reason fully 3-D finite strain constitutive equations are possible to be adopted without any condensation. This is a remarkable feature and up to our knowledge makes our model the first rod formulation as to permit general 3-D material laws for arbitrarily large strains. The present assumptions provide a consistent basis to the computational simulation of profile (distortional) deformations, which are typical of cold-formed thin-walled rod structures, and we believe this is one of the main contributions of our work. Several other examples presented in [5] further illustrate the robustness of the formulation.

Acknowledgements

First author acknowledges the University of São Paulo. Material support from IBNM (*Institut für Baumechanik und Numerische Mechanik*) of the Leibniz University of Hannover and from FAPESP (*Fundação de Amparo à Pesquisa do Estado de São Paulo*) under the grant 05/52453-2 are gratefully acknowledged by the second and third authors. Second author also acknowledges fellowship funding from CNPq (*Conselho Nacional de Desenvolvimento Tecnológico*) under the grant 305822/2006-3 and the *Mercator Gastprofessur* from DFG (*Deutsche Forschungsgemeinschaft*), which made possible his stay at the IBNM on a leave from the University of São Paulo.

References

[1] Pimenta, P.M. & Yojo, T., Geometrically-exact analysis of spatial frames. *Appl Mech Reviews, ASME*, **46(11)**, pp. 118–128, 1993.

[2] Pimenta, P.M., On a geometrically-exact finite-strain rod model. *Proceedings of the 3rd Pan-American Congress on Applied Mechanics, III PACAM*, São Paulo, 1993.

[3] Campello, E.M.B., *Análise não-linear de perfis metálicos conformados a frio*. Master's thesis, Escola Politécnica da Universidade de São Paulo, São Paulo, 2000. (in portuguese).

[4] Pimenta, P.M. & Campello, E.M.B., Geometrically nonlinear analysis of thin-walled space frames. *Proceedings of the Second European Conference on Computational Mechanics, II ECCM*, Cracow, 2001.

[5] Pimenta, P.M., Dasambiagio, E.R. & Campello, E.M.B., A truly finite strain rod model and its finite element implementation. *Submitted to journal Comput Meth Appl Mech Engrg*, 2009.

[6] Pimenta, P.M. & Campello, E.M.B., A fully nonlinear multi-parameter rod model incorporating general cross-sectional in-plane changes and out-of-plane warping. *Lat Amer J Solid Struct*, **1(1)**, pp. 119–140, 2003.

[7] Pimenta, P.M., Geometrically exact analysis of initially curved rods. *Advances in Computational Techniques for Structural Engineering*, Edinburgh, volume 1, pp. 99–108, 1996.

[8] Pimenta, P.M. & Campello, E.M.B., Shell curvature as an initial deformation: A geometrically-exact finite element approach. *Int J Numer Meth Engrg*, 2009. Published online, DOI 10.1002/nme.2528.

[9] Simo, J.C., A finite strain beam formulation. part I: The three-dimensional dynamic problem. *Comput Meth Appl Mech Engrg*, **49**, pp. 55–70, 1985.

[10] Simo, J.C. & Vu-Quoc, L., A three-dimesional finite strain rod model. part II: Computational aspects. *Comput Meth Appl Mech Engrg*, **58**, pp. 79–116, 1986.

[11] Cardona, A. & Geradin, M., A beam finite element non-linear theory with finite rotations. *Int J Numer Meth Engrg*, **26**, pp. 2403–38, 1988.

[12] Simo, J.C. & Vu-Quoc, L., A geometrically exact rod model incorporating shear and torsion-warping deformation. *Int J Solid Structures*, **27**, pp. 371–393, 1991.

[13] Ibrahimbegović, A. & Taylor, R.L., On the role of frame-invariance in structural mechanics models at finite rotations. *Comp Meth Appl Mech Engrg*, **191**, pp. 5159–5176, 2002.

[14] Crisfield, M.A. & Jelenić, G., Objectivity of strain measures in the geometrically-exact three-dimensional

beam theory and its finite element implementation. *Proc R Soc Lond*, **455**, pp. 1125–1147, 1999.
[15] Gruttmann, F. & Wagner, W., Geometrical and material nonlinear three-dimensional beams – theory and numerics. *Proceedings of the ECCM'99*, ed. W. Wunderlich, Munich, 1999.
[16] Jelenic, G. & Saje, M., A kinematically exact space finite strain beam model – finite element formulation by generalized virtual work principle. *Comput Meth Appl Mech Engrg*, **120**, pp. 131–161, 1995.
[17] Betsch, P. & Steinmann, P., Frame-indifferent beam finite elements based upon the geometrically-exact beam theory. *Int J Numer Methods Engrg*, **54**, pp. 1775–1788, 2002.
[18] Gruttmann, F., Sauer, R. & Wagner, W., A geometrical nonlinar eccentric 3D beam element with arbitrary cross-sections. *Comput Meth Appl Mech Engrg*, **160**, pp. 383–400, 1998.
[19] Bertram, A., *Elasticity and Plasticity of Large Deformations – An Introduction*. Springer-Verlag: Berlin-Heidelberg-New York, 2005.
[20] Ciarlet, P.J., *Mathematical Elasticity*, volume 1. North Holland, Amsterdam, 1988.
[21] Simo, J.C. & Hughes, T.J.R., *Computational Inelasticity*. Springer-Verlag: New York, 1998.

Appendix A

Tangent operator $\bar{\boldsymbol{G}}$ in (57) has the following structure

$$\bar{\boldsymbol{G}} = \begin{bmatrix} \boldsymbol{O} & \boldsymbol{O} & \boldsymbol{G}^{u'\theta} \\ \boldsymbol{O} & \boldsymbol{O} & \boldsymbol{G}^{\theta'\theta} \\ \boldsymbol{G}^{\theta u'} & \boldsymbol{G}^{\theta\theta'} & \boldsymbol{G}^{\theta\theta} \end{bmatrix} . \tag{86}$$

In order to derive the elements of (86), the following result is obtained by differentiation

$$\frac{\partial(\boldsymbol{\Gamma}^T \boldsymbol{t})}{\partial \boldsymbol{\theta}} = \boldsymbol{\Gamma}^T \frac{\partial \boldsymbol{t}}{\partial \boldsymbol{\theta}} + \boldsymbol{V}(\boldsymbol{\theta}, \boldsymbol{t}) \ , \tag{87}$$

where $\boldsymbol{t}$ is a generic vector and

$$\begin{aligned} \boldsymbol{V}(\boldsymbol{\theta}, \boldsymbol{t}) = {} & h_2(\theta)\,\boldsymbol{T} + h_3(\theta)\,(\boldsymbol{T\Theta} - 2\boldsymbol{\Theta T}) + \\ & -h_4(\theta)\,(\boldsymbol{\Theta t} \otimes \boldsymbol{\theta}) + h_5(\theta)\left(\boldsymbol{\Theta}^2 \boldsymbol{t} \otimes \boldsymbol{\theta}\right) \ , \end{aligned} \tag{88}$$

with $\boldsymbol{T} = \text{skew}(\boldsymbol{t})$. One can show that property

$$\boldsymbol{V}(\boldsymbol{\theta}, \boldsymbol{t}) = \boldsymbol{V}^T(\boldsymbol{\theta}, \boldsymbol{t}) + \boldsymbol{\Gamma}^T \boldsymbol{T} \boldsymbol{\Gamma} \tag{89}$$

holds for $\boldsymbol{V}(\boldsymbol{\theta}, \boldsymbol{t})$, and this is a crucial result in proving the symmetry of (86). With the aid of (87) and (88) it is possible to write

$$\begin{aligned} \boldsymbol{G}^{u'\theta} &= \left(\boldsymbol{G}^{\theta u'}\right)^T = -\boldsymbol{N\Gamma} \ , \\ \boldsymbol{G}^{\theta\theta'} &= \left(\boldsymbol{G}^{\theta'\theta}\right)^T = \boldsymbol{V}(\boldsymbol{\theta},\ \boldsymbol{m}) \quad \text{and} \\ \boldsymbol{G}^{\theta\theta} &= \left(\boldsymbol{G}^{\theta\theta}\right)^T = \boldsymbol{\Gamma}^T \boldsymbol{Z}' \boldsymbol{N\Gamma} - \boldsymbol{V}(\boldsymbol{\theta},\ \boldsymbol{z}' \times \boldsymbol{n}) + \boldsymbol{V}'(\boldsymbol{\theta},\ \boldsymbol{\theta}',\ \boldsymbol{m}) - \boldsymbol{\Gamma}'^{\mathrm{T}} \boldsymbol{M\Gamma} \ , \end{aligned} \tag{90}$$

in which $\boldsymbol{N} = \text{Skew}(\boldsymbol{n})$, $\boldsymbol{M} = S\text{kew}(\boldsymbol{m})$ and

$$\begin{aligned}\boldsymbol{V}'(\boldsymbol{\theta},\ \boldsymbol{\theta}',\ \boldsymbol{m}) = {} & h_3(\theta)(\boldsymbol{M\Theta}' - 2\boldsymbol{\Theta}'\boldsymbol{M}) - h_4(\theta)(\boldsymbol{\Theta}'\boldsymbol{m}\otimes\boldsymbol{\theta} + \boldsymbol{\Theta m}\otimes\boldsymbol{\theta}_{,\alpha}) + \\ & + h_5(\theta)\left((\boldsymbol{\Theta}'\boldsymbol{\Theta} + \boldsymbol{\Theta\Theta}')\boldsymbol{m}\otimes\boldsymbol{\theta} + \boldsymbol{\Theta}^2\boldsymbol{m}\otimes\boldsymbol{\theta}'\right) + \\ & + (\boldsymbol{\theta}\cdot\boldsymbol{\theta}')\left[h_4(\theta)\boldsymbol{M} + h_5(\theta)(\boldsymbol{M\Theta} - 2\boldsymbol{\Theta M})\right] + \\ & + (\boldsymbol{\theta}\cdot\boldsymbol{\theta}')\left[-h_6(\theta)(\boldsymbol{\Theta m}\otimes\boldsymbol{\theta}) + h_7(\theta)\left(\boldsymbol{\Theta}^2\boldsymbol{m}\otimes\boldsymbol{\theta}\right)\right] \ .\end{aligned}$$

Here the following trigonometric functions have been introduced

$$h_6(\theta) = \frac{h_3(\theta) - h_2(\theta) - 4h_4(\theta)}{\theta^2} \quad \text{and} \quad h_7(\theta) = \frac{h_4(\theta) - 5h_5(\theta)}{\theta^2} \ . \qquad (91^5)$$

Appendix B

Tangent operator $\boldsymbol{D}$ in (57) has following structure

$$\boldsymbol{D} = \begin{bmatrix} \dfrac{\partial \boldsymbol{n}^r}{\partial \boldsymbol{\eta}^r} & \dfrac{\partial \boldsymbol{n}^r}{\partial \boldsymbol{\kappa}^r} & \dfrac{\partial \boldsymbol{n}^r}{\partial \boldsymbol{p}} & \dfrac{\partial \boldsymbol{n}^r}{\partial \boldsymbol{p}'} & \dfrac{\partial \boldsymbol{n}^r}{\partial \boldsymbol{r}} & \dfrac{\partial \boldsymbol{n}^r}{\partial \boldsymbol{r}'} \\ \dfrac{\partial \boldsymbol{m}^r}{\partial \boldsymbol{\eta}^r} & \dfrac{\partial \boldsymbol{m}^r}{\partial \boldsymbol{\kappa}^r} & \dfrac{\partial \boldsymbol{m}^r}{\partial \boldsymbol{p}} & \dfrac{\partial \boldsymbol{m}^r}{\partial \boldsymbol{p}'} & \dfrac{\partial \boldsymbol{m}^r}{\partial \boldsymbol{r}} & \dfrac{\partial \boldsymbol{m}^r}{\partial \boldsymbol{r}'} \\ \dfrac{\partial \boldsymbol{\pi}}{\partial \boldsymbol{\eta}^r} & \dfrac{\partial \boldsymbol{\pi}}{\partial \boldsymbol{\kappa}^r} & \dfrac{\partial \boldsymbol{\pi}}{\partial \boldsymbol{p}} & \dfrac{\partial \boldsymbol{\pi}}{\partial \boldsymbol{p}'} & \dfrac{\partial \boldsymbol{\pi}}{\partial \boldsymbol{r}} & \dfrac{\partial \boldsymbol{\pi}}{\partial \boldsymbol{r}'} \\ \dfrac{\partial \boldsymbol{\alpha}}{\partial \boldsymbol{\eta}^r} & \dfrac{\partial \boldsymbol{\alpha}}{\partial \boldsymbol{\kappa}^r} & \dfrac{\partial \boldsymbol{\alpha}}{\partial \boldsymbol{p}} & \dfrac{\partial \boldsymbol{\alpha}}{\partial \boldsymbol{p}'} & \dfrac{\partial \boldsymbol{\alpha}}{\partial \boldsymbol{r}} & \dfrac{\partial \boldsymbol{\alpha}}{\partial \boldsymbol{r}'} \\ \dfrac{\partial \boldsymbol{\rho}}{\partial \boldsymbol{\eta}^r} & \dfrac{\partial \boldsymbol{\rho}}{\partial \boldsymbol{\kappa}^r} & \dfrac{\partial \boldsymbol{\rho}}{\partial \boldsymbol{p}} & \dfrac{\partial \boldsymbol{\rho}}{\partial \boldsymbol{p}'} & \dfrac{\partial \boldsymbol{\rho}}{\partial \boldsymbol{r}} & \dfrac{\partial \boldsymbol{\rho}}{\partial \boldsymbol{r}'} \\ \dfrac{\partial \boldsymbol{\beta}}{\partial \boldsymbol{\eta}^r} & \dfrac{\partial \boldsymbol{\beta}}{\partial \boldsymbol{\kappa}^r} & \dfrac{\partial \boldsymbol{\beta}}{\partial \boldsymbol{p}} & \dfrac{\partial \boldsymbol{\beta}}{\partial \boldsymbol{p}'} & \dfrac{\partial \boldsymbol{\beta}}{\partial \boldsymbol{r}} & \dfrac{\partial \boldsymbol{\beta}}{\partial \boldsymbol{r}'} \end{bmatrix} \ . \qquad (92)$$

The elements of (92) are displayed next.

[5] The singularities in $h_6(\theta)$ and $h_7(\theta)$ are also removable.

$$
\begin{aligned}
\frac{\partial \boldsymbol{n}^r}{\partial \boldsymbol{\eta}^r} &= \int_A \boldsymbol{C}_{33} dA \,, \\
\frac{\partial \boldsymbol{n}^r}{\partial \boldsymbol{\kappa}^r} &= -\int_A \boldsymbol{C}_{33} \boldsymbol{Y}^r dA \,, \\
\frac{\partial \boldsymbol{n}^r}{\partial \boldsymbol{p}} &= \int_A \left[\boldsymbol{C}_{3\alpha}\left(\boldsymbol{e}_3^r \otimes \boldsymbol{\psi}_{,\alpha}\right) + \left(\boldsymbol{C}_{33}\left(\boldsymbol{\kappa}^r \times \boldsymbol{e}_3^r\right)\right) \otimes \boldsymbol{\psi}\right] dA \,, \\
\frac{\partial \boldsymbol{n}^r}{\partial \boldsymbol{p}'} &= \int_A \boldsymbol{C}_{33}\left(\boldsymbol{e}_3^r \otimes \boldsymbol{\psi}\right) dA \,, \\
\frac{\partial \boldsymbol{n}^r}{\partial \boldsymbol{r}} &= \int_A \left[\left(\boldsymbol{C}_{3\gamma} \boldsymbol{e}_\beta^r\right) \otimes \boldsymbol{\phi}_{\beta,\gamma} + \left(\boldsymbol{C}_{33}\left(\boldsymbol{\kappa}^r \times \boldsymbol{e}_\beta^r\right)\right) \otimes \boldsymbol{\phi}_\beta\right] dA \,, \\
\frac{\partial \boldsymbol{n}^r}{\partial \boldsymbol{r}'} &= \int_A \left(\boldsymbol{C}_{33} \boldsymbol{e}_\beta^r\right) \otimes \boldsymbol{\phi}_\beta dA \,, \\
\frac{\partial \boldsymbol{m}^r}{\partial \boldsymbol{\eta}^r} &= \int_A \boldsymbol{Y}^r \boldsymbol{C}_{33} dA \,, \\
\frac{\partial \boldsymbol{m}^r}{\partial \boldsymbol{\kappa}^r} &= -\int_A \boldsymbol{Y}^r \boldsymbol{C}_{33} \boldsymbol{Y}^r dA \,, \\
\frac{\partial \boldsymbol{m}^r}{\partial \boldsymbol{p}} &= \int_A \left[\left(\boldsymbol{Y}^r \boldsymbol{C}_{3\alpha} \boldsymbol{e}_3^r\right) \otimes \boldsymbol{\psi}_{,\alpha} + \left(\boldsymbol{Y}^r \boldsymbol{C}_{33}\left(\boldsymbol{\kappa}^r \times \boldsymbol{e}_3^r\right)\right) \otimes \boldsymbol{\psi} + \left(\boldsymbol{e}_3^r \times \boldsymbol{\tau}_3^r\right) \otimes \boldsymbol{\psi}\right] dA \,, \qquad (93) \\
\frac{\partial \boldsymbol{m}^r}{\partial \boldsymbol{p}'} &= \int_A \left(\boldsymbol{Y}^r \boldsymbol{C}_{33} \boldsymbol{e}_3^r\right) \otimes \boldsymbol{\psi} dA \,, \\
\frac{\partial \boldsymbol{m}^r}{\partial \boldsymbol{r}} &= \int_A \left[\left(\boldsymbol{Y}^r \boldsymbol{C}_{3\gamma} \boldsymbol{e}_\beta^r\right) \otimes \boldsymbol{\phi}_{\beta,\gamma} + \left(\boldsymbol{Y}^r \boldsymbol{C}_{33}\left(\boldsymbol{\kappa}^r \times \boldsymbol{e}_\beta^r\right)\right) \otimes \boldsymbol{\phi}_\beta + \left(\boldsymbol{e}_\beta^r \times \boldsymbol{\tau}_3^r\right) \otimes \boldsymbol{\phi}_\beta\right] dA \,, \\
\frac{\partial \boldsymbol{m}^r}{\partial \boldsymbol{r}'} &= \int_A \left(\boldsymbol{Y}^r \boldsymbol{C}_{33} \boldsymbol{e}_\beta^r\right) \otimes \boldsymbol{\phi}_\beta dA \,, \\
\frac{\partial \boldsymbol{\pi}}{\partial \boldsymbol{\eta}^r} &= \int_A \left[\boldsymbol{\psi}_{,\alpha} \otimes \left(\boldsymbol{C}_{\alpha 3}^T \boldsymbol{e}_3^r\right) + \boldsymbol{\psi} \otimes \left(\boldsymbol{C}_{33}^T\left(\boldsymbol{\kappa}^r \times \boldsymbol{e}_3^r\right)\right)\right] dA \,, \\
\frac{\partial \boldsymbol{\pi}}{\partial \boldsymbol{\kappa}^r} &= \int_A \left[\boldsymbol{\psi}_{,\alpha} \otimes \left(\boldsymbol{Y}^r \boldsymbol{C}_{\alpha 3}^T \boldsymbol{e}_3^r\right) + \boldsymbol{\psi} \otimes \left(\boldsymbol{Y}^r \boldsymbol{C}_{33}^T\left(\boldsymbol{\kappa}^r \times \boldsymbol{e}_3^r\right)\right) + \boldsymbol{\psi} \otimes \left(\boldsymbol{e}_3^r \times \boldsymbol{\tau}_3^r\right)\right] dA \,, \\
\frac{\partial \boldsymbol{\pi}}{\partial \boldsymbol{p}} &= \int_A \left[\left(\boldsymbol{e}_3^r \cdot \boldsymbol{C}_{\alpha\beta} \boldsymbol{e}_3^r\right)\left(\boldsymbol{\psi}_{,\alpha} \otimes \boldsymbol{\psi}_{,\beta}\right) + \left(\boldsymbol{e}_3^r \cdot \boldsymbol{C}_{\alpha 3}\left(\boldsymbol{\kappa}^r \times \boldsymbol{e}_3^r\right)\right)\left(\boldsymbol{\psi}_{,\alpha} \otimes \boldsymbol{\psi}\right)\right] dA + \\
&\quad + \int_A \boldsymbol{\psi} \otimes \left(\boldsymbol{\kappa}^r \times \boldsymbol{e}_3^r\right)\left[\boldsymbol{C}_{3\alpha}\left(\boldsymbol{e}_3^r \otimes \boldsymbol{\psi}_{,\alpha}\right) + \boldsymbol{C}_{33}\left(\boldsymbol{\kappa}^r \times \boldsymbol{e}_3^r\right) \otimes \boldsymbol{\psi}\right] dA \,, \\
\frac{\partial \boldsymbol{\pi}}{\partial \boldsymbol{p}'} &= \int_A \left[\left(\boldsymbol{\psi}_{,\alpha} \otimes \boldsymbol{e}_3^r\right) \boldsymbol{C}_{\alpha 3}\left(\boldsymbol{e}_3^r \otimes \boldsymbol{\psi}\right) + \boldsymbol{\psi} \otimes \left(\boldsymbol{\kappa}^r \times \boldsymbol{e}_3^r\right) \boldsymbol{C}_{33}\left(\boldsymbol{e}_3^r \otimes \boldsymbol{\psi}\right)\right] dA \,,
\end{aligned}
$$

$$
\begin{aligned}
\frac{\partial \boldsymbol{\pi}}{\partial \boldsymbol{r}} &= \int_A \left(\boldsymbol{\psi}_{,\alpha} \otimes \boldsymbol{e}_3^r\right) \left[\boldsymbol{C}_{\alpha\gamma} \left(\boldsymbol{e}_\beta^r \otimes \boldsymbol{\phi}_{\beta,\gamma}\right) + \boldsymbol{C}_{\alpha 3} \left(\boldsymbol{\kappa}^r \times \boldsymbol{e}_\beta^r\right) \otimes \boldsymbol{\phi}_\beta\right] dA + \\
&\quad + \int_A \boldsymbol{\psi} \otimes \left(\boldsymbol{\kappa}^r \times \boldsymbol{e}_3^r\right) \left[\boldsymbol{C}_{3\gamma} \left(\boldsymbol{e}_\beta^r \otimes \boldsymbol{\phi}_{\beta,\gamma}\right) + \boldsymbol{C}_{33} \left(\boldsymbol{\kappa}^r \times \boldsymbol{e}_\beta^r\right) \otimes \boldsymbol{\phi}_\beta\right] dA \, , \\
\frac{\partial \boldsymbol{\pi}}{\partial \boldsymbol{r}'} &= \int_A \left[\left(\boldsymbol{\psi}_{,\alpha} \otimes \boldsymbol{e}_3^r\right) \boldsymbol{C}_{\alpha 3} \left(\boldsymbol{e}_\beta^r \otimes \boldsymbol{\phi}_\beta\right) + \boldsymbol{\psi} \otimes \left(\boldsymbol{\kappa}^r \times \boldsymbol{e}_3^r\right) \boldsymbol{C}_{33} \left(\boldsymbol{e}_\beta^r \otimes \boldsymbol{\phi}_\beta\right)\right] dA \, , \\
\frac{\partial \boldsymbol{\alpha}}{\partial \boldsymbol{\eta}^r} &= \int_A \left(\boldsymbol{\psi} \otimes \boldsymbol{e}_3^r\right) \boldsymbol{C}_{33} dA \, , \\
\frac{\partial \boldsymbol{\alpha}}{\partial \boldsymbol{\kappa}^r} &= -\int_A \left(\boldsymbol{\psi} \otimes \boldsymbol{e}_3^r\right) \boldsymbol{C}_{33} \boldsymbol{Y}^r dA \, , \\
\frac{\partial \boldsymbol{\alpha}}{\partial \boldsymbol{p}} &= \int_A \left(\boldsymbol{\psi} \otimes \boldsymbol{e}_3^r\right) \left[\boldsymbol{C}_{3\alpha} \left(\boldsymbol{e}_3^r \otimes \boldsymbol{\psi}_{,\alpha}\right) + \boldsymbol{C}_{33} \left(\boldsymbol{\kappa}^r \times \boldsymbol{e}_3^r\right) \otimes \boldsymbol{\psi}\right] dA \, , \\
\frac{\partial \boldsymbol{\alpha}}{\partial \boldsymbol{p}'} &= \int_A \left(\boldsymbol{\psi} \otimes \boldsymbol{e}_3^r\right) \boldsymbol{C}_{33} \left(\boldsymbol{e}_3^r \otimes \boldsymbol{\psi}\right) dA \, , \\
\frac{\partial \boldsymbol{\alpha}}{\partial \boldsymbol{r}} &= \int_A \left(\boldsymbol{\psi} \otimes \boldsymbol{e}_3^r\right) \left[\boldsymbol{C}_{3\gamma} \left(\boldsymbol{e}_\beta^r \otimes \boldsymbol{\phi}_{\beta,\gamma}\right) + \boldsymbol{C}_{33} \left(\boldsymbol{\kappa}^r \times \boldsymbol{e}_\beta^r\right) \otimes \boldsymbol{\phi}_\beta\right] dA \, , \\
\frac{\partial \boldsymbol{\alpha}}{\partial \boldsymbol{r}'} &= \int_A \left(\boldsymbol{\psi} \otimes \boldsymbol{e}_3^r\right) \boldsymbol{C}_{33} \left(\boldsymbol{e}_\beta^r \otimes \boldsymbol{\phi}_\beta\right) dA \, , \\
\frac{\partial \boldsymbol{\rho}}{\partial \boldsymbol{\eta}^r} &= \int_A \left[\left(\boldsymbol{\phi}_{\delta,\alpha} \otimes \boldsymbol{e}_\delta^r\right) \boldsymbol{C}_{\alpha 3} + \boldsymbol{\phi}_\delta \otimes \left(\boldsymbol{\kappa}^r \times \boldsymbol{e}_\delta^r\right) \boldsymbol{C}_{33}\right] dA \, , \\
\frac{\partial \boldsymbol{\rho}}{\partial \boldsymbol{\kappa}^r} &= \int_A \left[-\left(\boldsymbol{\phi}_{\delta,\alpha} \otimes \boldsymbol{e}_\delta^r\right) \boldsymbol{C}_{\alpha 3} \boldsymbol{Y}^r - \boldsymbol{\phi}_\delta \otimes \left(\boldsymbol{\kappa}^r \times \boldsymbol{e}_\delta^r\right) \boldsymbol{C}_{33} \boldsymbol{Y}^r + \boldsymbol{\phi}_\beta \otimes \left(\boldsymbol{e}_\beta^r \times \boldsymbol{\tau}_3^r\right)\right] dA \, , \\
\frac{\partial \boldsymbol{\rho}}{\partial \boldsymbol{p}} &= \int_A \left(\boldsymbol{\phi}_{\delta,\alpha} \otimes \boldsymbol{e}_\delta^r\right) \left[\boldsymbol{C}_{\alpha\beta} \left(\boldsymbol{e}_3^r \otimes \boldsymbol{\psi}_{,\beta}\right) + \boldsymbol{C}_{\alpha 3} \left(\left(\boldsymbol{\kappa}^r \times \boldsymbol{e}_3^r\right) \otimes \boldsymbol{\psi}\right)\right] dA + \\
&\quad + \int_A \boldsymbol{\phi}_\delta \otimes \left(\boldsymbol{\kappa}^r \times \boldsymbol{e}_\delta^r\right) \left[\boldsymbol{C}_{3\alpha} \left(\boldsymbol{e}_3^r \otimes \boldsymbol{\psi}_{,\alpha}\right) + \boldsymbol{C}_{33} \left(\boldsymbol{\kappa}^r \times \boldsymbol{e}_3^r\right) \otimes \boldsymbol{\psi}\right] dA \, , \\
\frac{\partial \boldsymbol{\rho}}{\partial \boldsymbol{p}'} &= \int_A \left[\left(\boldsymbol{\phi}_{\delta,\alpha} \otimes \boldsymbol{e}_\delta^r\right) \boldsymbol{C}_{\alpha 3} \left(\boldsymbol{e}_3^r \otimes \boldsymbol{\psi}\right) + \boldsymbol{\phi}_\delta \otimes \left(\boldsymbol{\kappa}^r \times \boldsymbol{e}_\delta^r\right) \boldsymbol{C}_{33} \left(\boldsymbol{e}_3^r \otimes \boldsymbol{\psi}\right)\right] dA \, , \\
\frac{\partial \boldsymbol{\rho}}{\partial \boldsymbol{r}} &= \int_A \left(\boldsymbol{\phi}_{\delta,\alpha} \otimes \boldsymbol{e}_\delta^r\right) \left[\boldsymbol{C}_{\alpha\gamma} \left(\boldsymbol{e}_\beta^r \otimes \boldsymbol{\phi}_{\beta,\gamma}\right) + \boldsymbol{C}_{\alpha 3} \left(\boldsymbol{\kappa}^r \times \boldsymbol{e}_\beta^r\right) \otimes \boldsymbol{\phi}_\beta\right] dA + \\
&\quad + \int_A \boldsymbol{\phi}_\delta \otimes \left(\boldsymbol{\kappa}^r \times \boldsymbol{e}_\delta^r\right) \left[\boldsymbol{C}_{3\gamma} \left(\boldsymbol{e}_\beta^r \otimes \boldsymbol{\phi}_{\beta,\gamma}\right) + \boldsymbol{C}_{33} \left(\boldsymbol{\kappa}^r \times \boldsymbol{e}_\beta^r\right) \otimes \boldsymbol{\phi}_\beta\right] dA \, , \\
\frac{\partial \boldsymbol{\rho}}{\partial \boldsymbol{r}'} &= \int_A \left[\left(\boldsymbol{\phi}_{\delta,\alpha} \otimes \boldsymbol{e}_\delta^r\right) \boldsymbol{C}_{\alpha 3} \left(\boldsymbol{e}_\beta^r \otimes \boldsymbol{\phi}_\beta\right) + \boldsymbol{\phi}_\delta \otimes \left(\boldsymbol{\kappa}^r \times \boldsymbol{e}_\delta^r\right) \boldsymbol{C}_{33} \left(\boldsymbol{e}_\beta^r \otimes \boldsymbol{\phi}_\beta\right)\right] dA \, , \\
\frac{\partial \boldsymbol{\beta}}{\partial \boldsymbol{\eta}^r} &= \int_A \left(\boldsymbol{\phi}_\beta \otimes \boldsymbol{e}_\beta^r\right) \boldsymbol{C}_{33} dA \, ,
\end{aligned}
\tag{94}
$$

Brazilian Society of Mechanical Sciences and Engineering, ISBN 978-85-85769-43-7

$$\begin{aligned}
\frac{\partial \boldsymbol{\beta}}{\partial \boldsymbol{\kappa}^r} &= -\int_A \left(\boldsymbol{\phi}_\beta \otimes \boldsymbol{e}^r_\beta\right) \boldsymbol{C}_{33} \boldsymbol{Y}^r dA \,, \\
\frac{\partial \boldsymbol{\beta}}{\partial \boldsymbol{p}} &= \int_A \left(\boldsymbol{\phi}_\beta \otimes \boldsymbol{e}^r_\beta\right) \left[\boldsymbol{C}_{3\alpha} \left(\boldsymbol{e}^r_3 \otimes \boldsymbol{\psi}_{,\alpha}\right) + \boldsymbol{C}_{33} \left(\boldsymbol{\kappa}^r \times \boldsymbol{e}^r_3\right) \otimes \boldsymbol{\psi}\right] dA \,, \\
\frac{\partial \boldsymbol{\beta}}{\partial \boldsymbol{p}'} &= \int_A \left(\boldsymbol{\phi}_\beta \otimes \boldsymbol{e}^r_\beta\right) \boldsymbol{C}_{33} \left(\boldsymbol{e}^r_3 \otimes \boldsymbol{\psi}\right) dA \,, \\
\frac{\partial \boldsymbol{\beta}}{\partial \boldsymbol{r}} &= \int_A \left(\boldsymbol{\phi}_\alpha \otimes \boldsymbol{e}^r_\alpha\right) \left[\boldsymbol{C}_{3\gamma} \left(\boldsymbol{e}^r_\beta \otimes \boldsymbol{\phi}_{\beta,\gamma}\right) + \boldsymbol{C}_{33} \left(\boldsymbol{\kappa}^r \times \boldsymbol{e}^r_\beta\right) \otimes \boldsymbol{\phi}_\beta\right] dA \quad \text{and} \\
\frac{\partial \boldsymbol{\beta}}{\partial \boldsymbol{r}'} &= \int_A \left(\boldsymbol{\phi}_\alpha \otimes \boldsymbol{e}^r_\alpha\right) \boldsymbol{C}_{33} \left(\boldsymbol{e}^r_\beta \otimes \boldsymbol{\phi}_\beta\right) dA \,.
\end{aligned} \tag{95}$$

Appendix C

Tangent operator $\boldsymbol{L}$ has following structure

$$\boldsymbol{L} = \begin{bmatrix}
\frac{\partial \bar{\boldsymbol{n}}}{\partial \boldsymbol{u}} & \frac{\partial \bar{\boldsymbol{n}}}{\partial \boldsymbol{\theta}} & \frac{\partial \bar{\boldsymbol{n}}}{\partial \boldsymbol{p}} & \frac{\partial \bar{\boldsymbol{n}}}{\partial \boldsymbol{r}} \\
\frac{\partial \bar{\boldsymbol{\mu}}}{\partial \boldsymbol{u}} & \frac{\partial \bar{\boldsymbol{\mu}}}{\partial \boldsymbol{\theta}} & \frac{\partial \bar{\boldsymbol{\mu}}}{\partial \boldsymbol{p}} & \frac{\partial \bar{\boldsymbol{\mu}}}{\partial \boldsymbol{r}} \\
\frac{\partial \bar{\boldsymbol{\alpha}}}{\partial \boldsymbol{u}} & \frac{\partial \bar{\boldsymbol{\alpha}}}{\partial \boldsymbol{\theta}} & \frac{\partial \bar{\boldsymbol{\alpha}}}{\partial \boldsymbol{p}} & \frac{\partial \bar{\boldsymbol{\alpha}}}{\partial \boldsymbol{r}} \\
\frac{\partial \bar{\boldsymbol{\beta}}}{\partial \boldsymbol{u}} & \frac{\partial \bar{\boldsymbol{\beta}}}{\partial \boldsymbol{\theta}} & \frac{\partial \bar{\boldsymbol{\beta}}}{\partial \boldsymbol{p}} & \frac{\partial \bar{\boldsymbol{\beta}}}{\partial \boldsymbol{r}}
\end{bmatrix} . \tag{96}$$

For instance, semi-tangential external moments are conservative moments characterized by the following time derivative

$$\dot{\bar{\boldsymbol{m}}} = \frac{1}{2} \boldsymbol{\omega} \times \bar{\boldsymbol{m}} \,. \tag{97}$$

For this type of loading the only nonzero submatrix of $\boldsymbol{L}$ is

$$\frac{\partial \bar{\boldsymbol{m}}}{\partial \boldsymbol{\theta}} = \mathrm{Sym}\left(\boldsymbol{V}\left(\boldsymbol{\theta}, \bar{\boldsymbol{m}}\right)\right) \,. \tag{98[6]}$$

In contrast, for a constant eccentric force $\bar{\boldsymbol{n}}$ whose moment is $\bar{\boldsymbol{m}} = \boldsymbol{s} \times \bar{\boldsymbol{n}}$ (with $\boldsymbol{s}$ as the eccentricity vector), this submatrix is given by

$$\frac{\partial \bar{\boldsymbol{m}}}{\partial \boldsymbol{\theta}} = \boldsymbol{\Gamma}^T \mathrm{Sym}\left(\boldsymbol{S}\bar{\boldsymbol{N}}\right) \boldsymbol{\Gamma} + \mathrm{Sym}\left(\boldsymbol{V}\left(\boldsymbol{\theta}, \bar{\boldsymbol{m}}\right)\right) \,, \tag{99}$$

where $\boldsymbol{S} = \mathrm{Skew}(\boldsymbol{s})$ and $\bar{\boldsymbol{N}} = \mathrm{Skew}(\bar{\boldsymbol{n}})$.

[6] The operator Sym $(\bullet)$ extracts the symmetric part of $(\bullet)$, i.e. $\mathrm{Sym} = \frac{1}{2}\left[(\bullet) + (\bullet)^T\right]$.